Measurement of cross sections and properties of the Higgs boson in decays to bosons using the ATLAS detector

Monica Trovatelli
University of Victoria (Canada)

DIS2018, Kobe 16-20 Apr 2018

Outline

- *Higgs physics in diboson final states*
  - *Overview of the (so far) ATLAS Run-2 measurements in WW*/ZZ*/γγ decay channels*

- *Higgs boson cross-sections, which?*
  - *Fiducial inclusive and Differential*
  - *Total (full phase-space)*
  - *Production-mode cross-section*

- *Other properties measurements:*
  - *Couplings*
  - *Mass*
  - *Width and Spin/Parity*

- *Remarks and Conclusions*

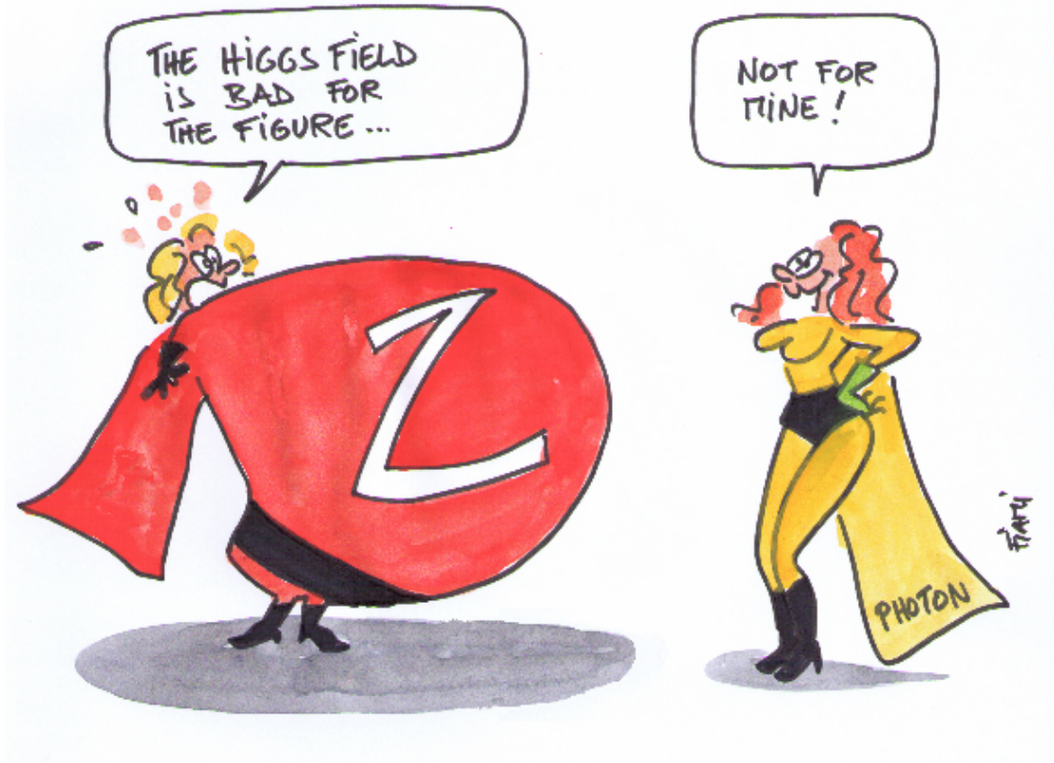

Higgs boson measurements in diboson final states

- Despite the **low branching fraction of H → WW*(→lνlν)/ZZ*/γγ**, these decays channels have a **clean signature** and constitute a **powerful tool for** many Higgs boson **properties measurements**

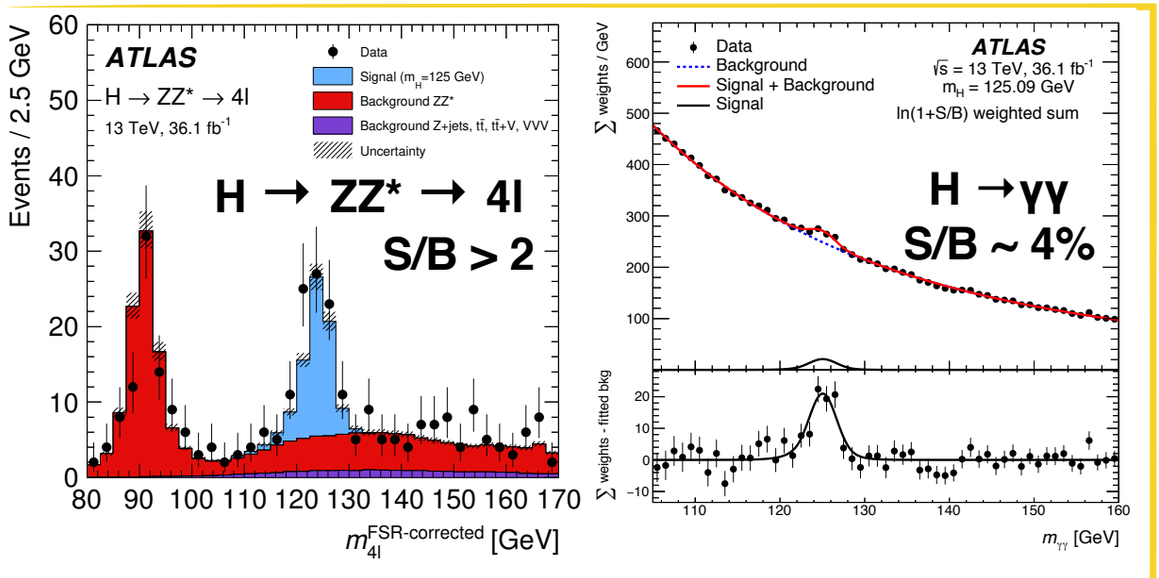

Fully reconstructed mass - clean peak

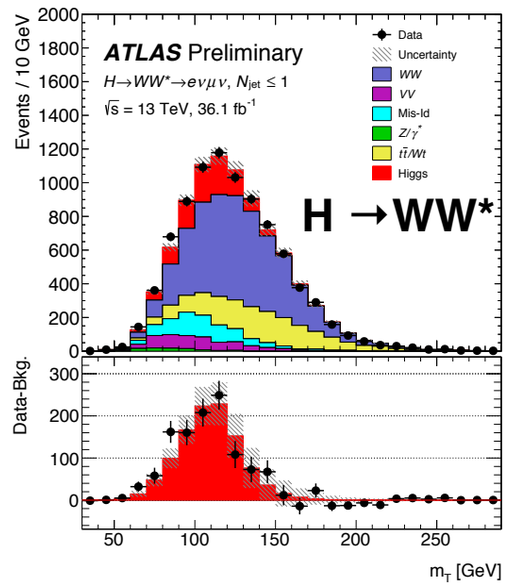

Larger BR ~ 1.5%
Clean signature
High background

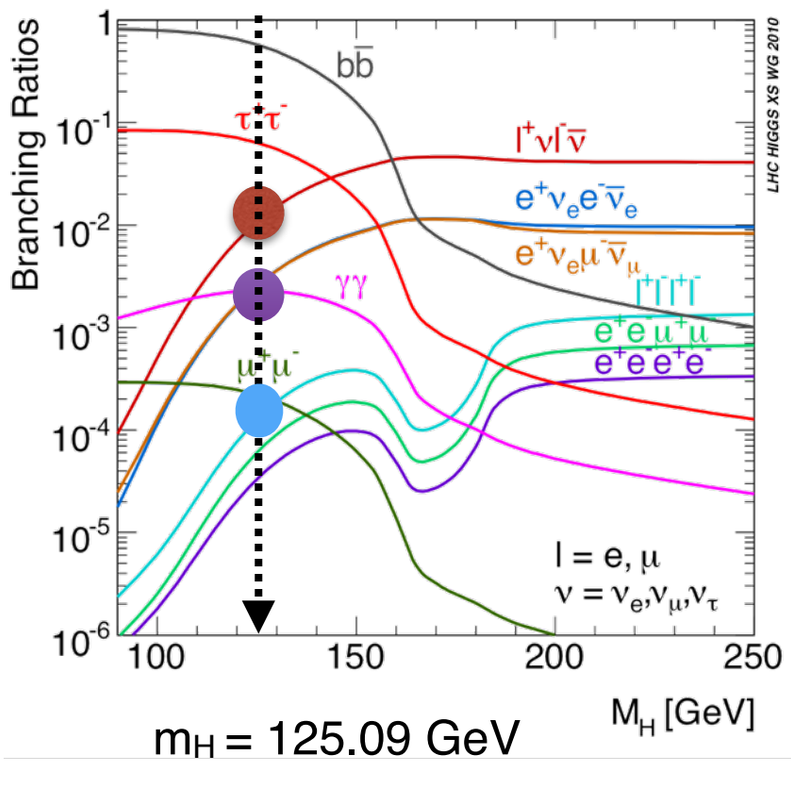

mH = 125.09 GeV

Run-II advantages for measurements

@13TeV $\sigma_{H,8TeV}$ x 2.3
36.1 fb^{-1} (2015+2016) analysed

Plenty of new ATLAS results already published:

	H→ZZ*→4ℓ	H→γγ	H→WW*	Combined(*)
Cross-sections	JHEP10(2017)132	arXiv:1802.04146	ATLAS-CONF-2018-004	ATLAS-CONF-2017-047 ATLAS-CONF-2018-002
Couplings	JHEP03(2018)095	arXiv:1802.04146	— — —	ATLAS-CONF-2017-047
Mass	— — —	— — —	— — —	ATLAS-CONF-2017-046

(*) currently combining only 4l and γγ channels

Higgs boson cross-section measurements

In Run-2 **different Higgs boson cross-section measurements** considered:

- **Inclusive fiducial and differential cross-section**
  - Measured in fiducial volume
    - Avoid model-dependent extrapolations → only correct for inefficiencies & reconstruction effects

$$\sigma_{i,fid} = \frac{N_{i,fit}}{L \times C_i}, C_i = \frac{N_{i,reco}}{N_{i,part}}$$

C_i = 50%(75%) for H4l(Hγγ)

    - Preserve measured results over years to allow comparison to future new theories
  - Inclusive: No attempt to separate Higgs production/decay modes → compare with best available predictions in the detector phase space
  - Differential: test Higgs boson kinematics and modelling with $p_T H$, $|yH|$, p_{Tj1}, Njet,…

also sensitive to BSM physics

- **Total cross-section:** extrapolate to full phase space and combine channels to improve precision
- **Production mode cross-section** (Simplified Template cross section framework* (STXS)):
  - *simple fiducial region definitions* matching specific experimental categories (ggF 0jets, etc..)
  - reduce theoretical uncertainties

(*) LHC Higgs X-Sec WG: : 4 [arXiv:1610.07922]

H→WW*→eνμν - Analysis

ATLAS-CONF-2018-004
Most recent result!
Not yet combined with others

Analysis strategy in brief

- **Signature**: two prompt isolated leptons and missing momentum

- **Events split in 3 major Signal Regions** on Njets(*):
  - **Njet = 0 and Njet = 1 (ggF dominated)**
    - m_T used as discriminant
  - **Njet ≥ 2 (VBF dominated)**
    - BDT used as discriminant

  } b-jet veto in all categories to reduce ttbar ($\sigma_{13\ TeV}/\sigma_{8\ TeV} \approx 3.3$)

- Irreducible backgrounds normalised to data via CRs
  - non-resonant WW, ttbar and Z→ττ
- Mis-identified leptons (~10% of total bkg) fully data-driven

(*) complete event selection table in backup

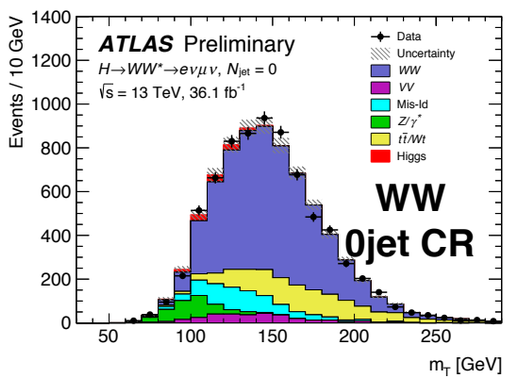

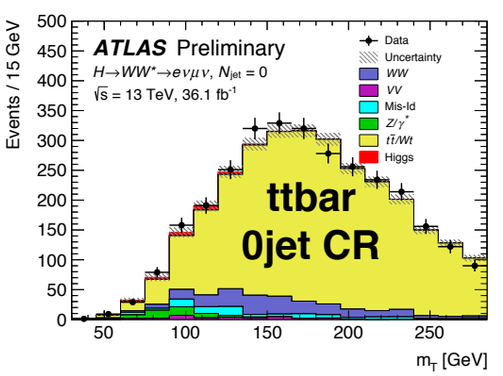

- Simultaneous SRs and CR max likelihood fit
  - **16 fits regions defined for Njet ≤ 1:**
    - Different bkg composition
    - Enhance sensitivity

$$[2 \times m_{\ell\ell}] \bullet [2 \times p_T^{sub-leading}] \bullet [e\mu / \mu e]$$

  - **4 BDT bins for VBF enriched category**
    - S(VBF)/B ~0.6 in the last bin

⇒ extract both ggF and VBF cross-sections

- Other production/decays modes fixed to SM

ggF: 6.3σ (exp. 5.2σ)

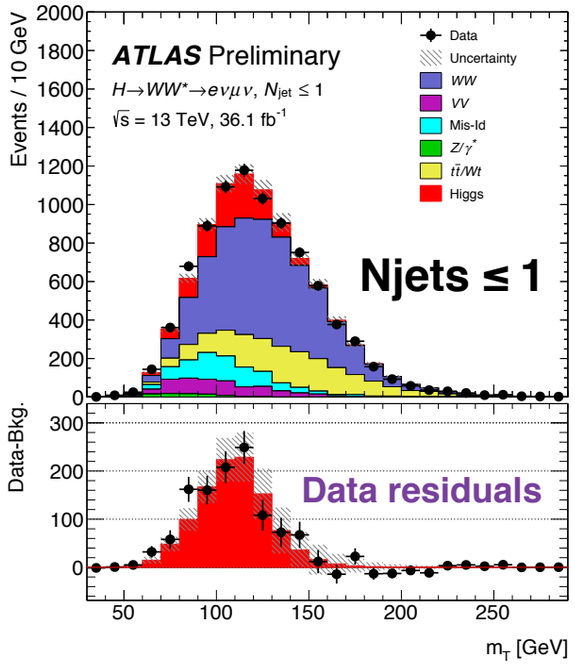

VBF: 1.9σ (exp. 2.7σ)

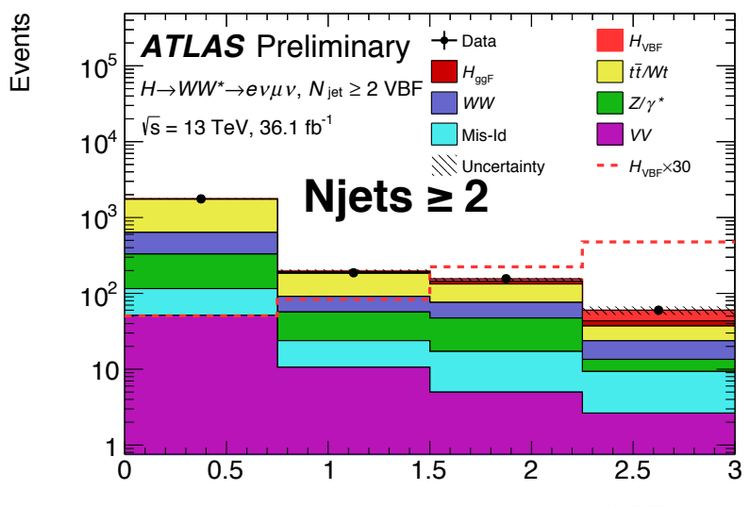

H→WW*→eνμν - Results

Signal strength and cross-section results:

	Run-2	Run-1
μ_{ggF}	$= 1.21^{+0.12}_{-0.11}(\mathrm{stat.})^{+0.18}_{-0.17}(\mathrm{sys.}) = 1.21^{+0.22}_{-0.21}$	$\mu_{ggF} = 1.02^{+0.29}_{-0.26}$
μ_{VBF}	$= 0.62^{+0.30}_{-0.28}(\mathrm{stat.}) \pm 0.22(\mathrm{sys.}) = 0.62^{+0.37}_{-0.36}$	$\mu_{VBF} = 1.27^{+0.53}_{-0.45}$

ggF: Precision improved by 36%
VBF: Limited due higher pile-up ⇒ higher bkg

$$\sigma_{\mathrm{ggF}} \cdot \mathcal{B}_{H\to WW^*} = 12.6^{+1.3}_{-1.2}(\mathrm{stat.})^{+1.9}_{-1.8}(\mathrm{sys.})\ \mathrm{pb} = 12.6^{+2.3}_{-2.1}\ \mathrm{pb}$$
$$\sigma_{\mathrm{VBF}} \cdot \mathcal{B}_{H\to WW^*} = 0.50^{+0.24}_{-0.23}(\mathrm{stat.}) \pm 0.18(\mathrm{sys.})\ \mathrm{pb} = 0.50^{+0.30}_{-0.29}\ \mathrm{pb}.$$

68% and 95% CL contours

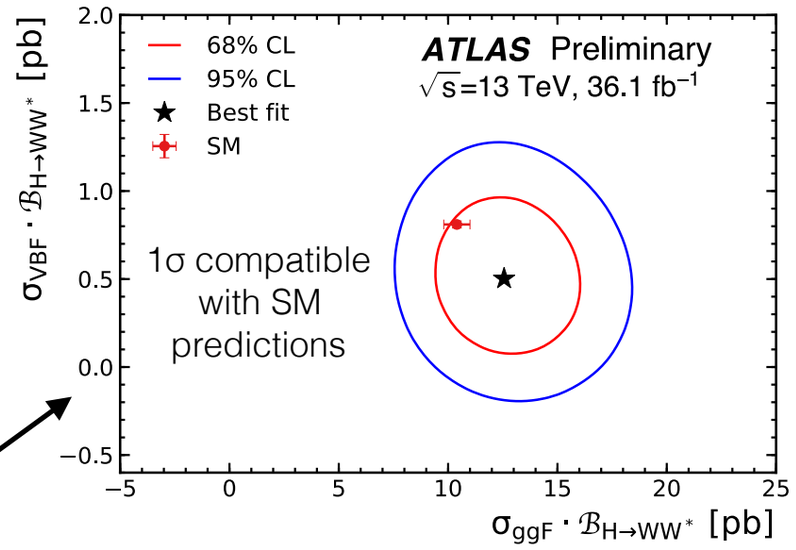

Uncertainties on the cross-sections measurement:

Significant uncertainties from Theory:
- ~5% on $\sigma_{(ggF)}$ due to WW background modelling
- 15% on $\sigma_{(VBF)}$ due to QCD scale on ggF in VBF phase space

Limited MC statistics important especially **in VBF**
$\sigma_{(ggF)}$ dominated by systematics (exp~theo)

precision of the measurements →

Source	$\frac{\Delta\sigma_{\mathrm{ggF}}}{\sigma_{\mathrm{ggF}}}$ [%]	$\frac{\Delta\sigma_{\mathrm{VBF}}}{\sigma_{\mathrm{VBF}}}$ [%]
Data statistics	±8	±46
CR statistics	±8	±9
MC statistics	±5	±23
Theoretical uncertainties	±8	±21
ggF signal	±5	±15
VBF signal	<1	±15
WW	±5	±12
Top-quark	±4	±4
Experimental uncertainties	±9	±8
b-tagging	±5	±6
Pile-up	±5	±2
Jet	±3	±4
Electron	±3	<1
Misidentified leptons	±5	±9
Luminosity	±2	±3
TOTAL	±17	±59

H→ZZ*→4ℓ inclusive and differential cross-section

JHEP10(2017)132

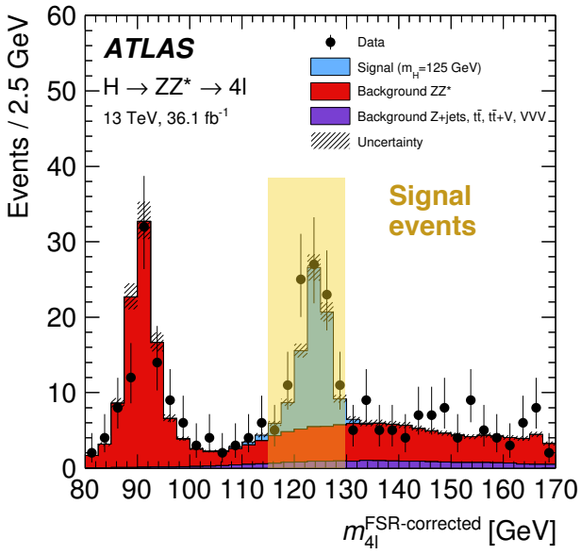

Fit m4l for each decay channel (**right**) or differential distributions (**below**) to extract N_{Signal}

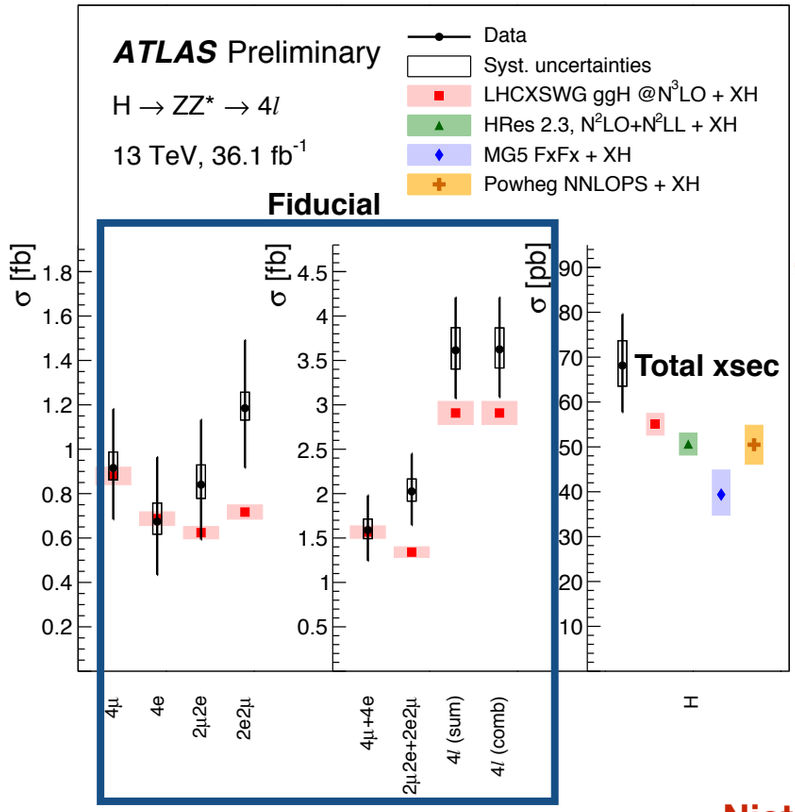

Combined inclusive fiducial xsec:

$$\sigma_{fid,comb} = 3.62 \pm 0.50(stat)^{+0.25}_{-0.20}(sys)\,fb$$

$$\sigma_{fid,SM} = 2.91 \pm 0.13\,fb$$

~15% precision

Good agreement with LHCXSWG prediction (1.3σ difference in mixed channels)

p_TH—> test perturbative QCD

|y4ℓ|—> test gluon PDFs

Njets—> test modelling of radiations at high pT, sensitive to prod modes

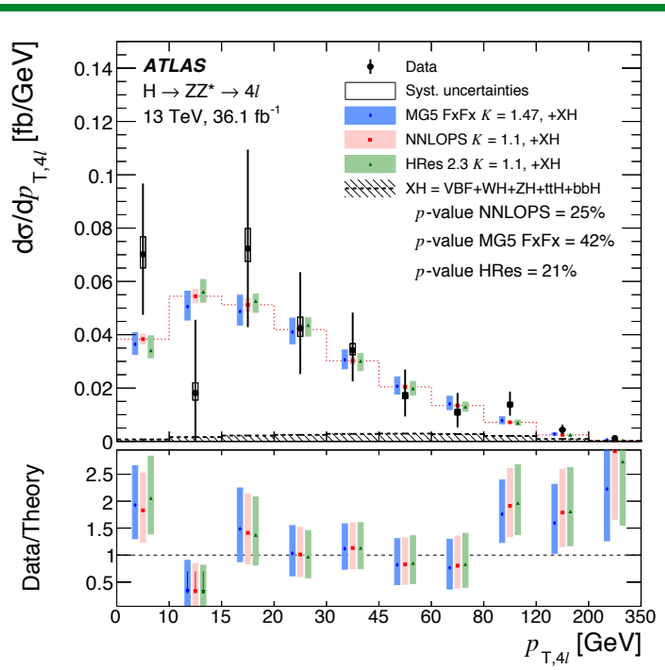

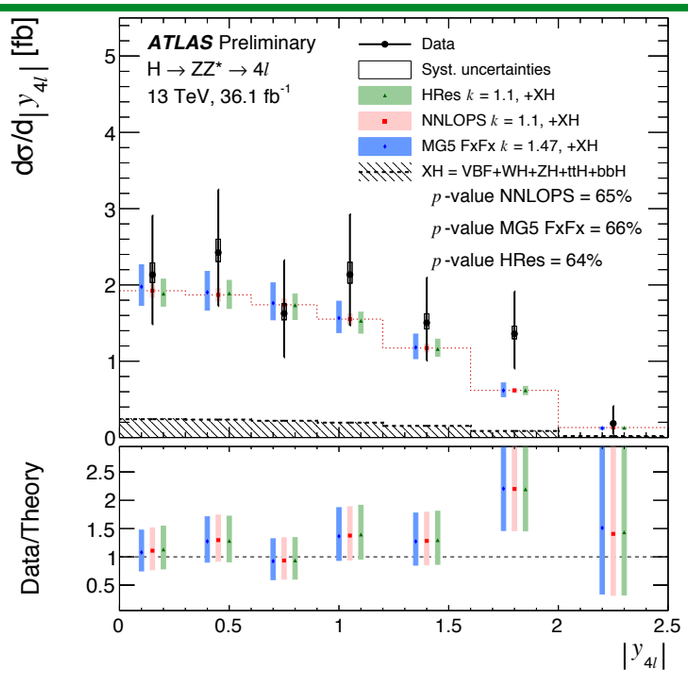

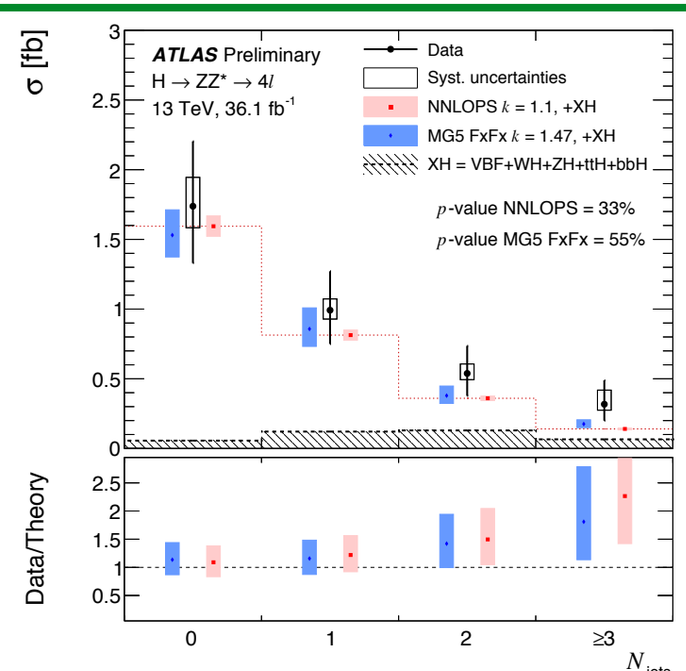

Overall good theoretical description of data. Precision statistically limited

arXiv:1802.04146

H→γγ inclusive and differential cross-section

Fit to mγγ distribution to extract N_{Signal}: **1) inclusively** in production mode **2)** in each **production mode-enhanced region** or differential distribution

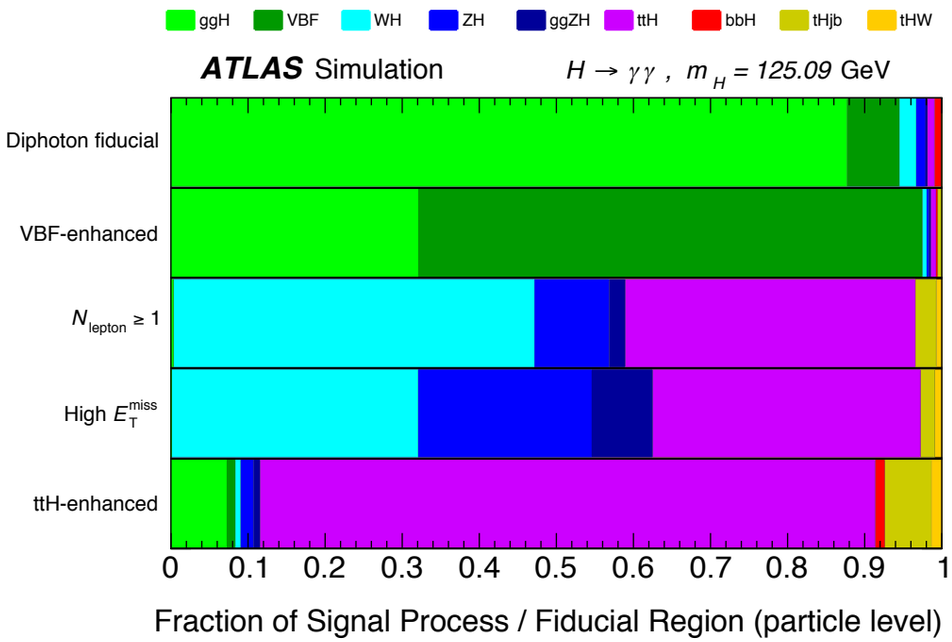

measured xsections

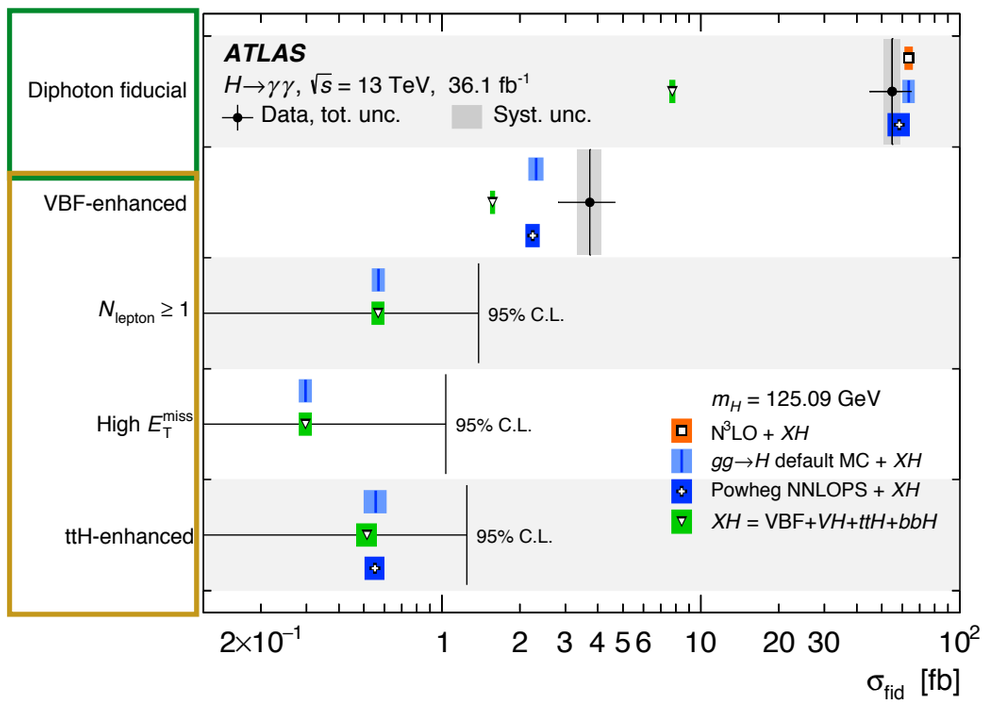

Differential and double differential measurements

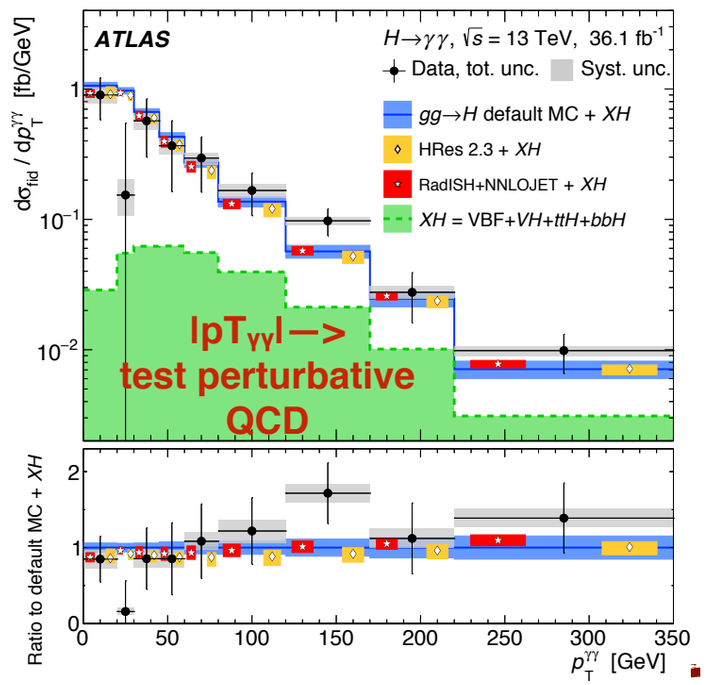

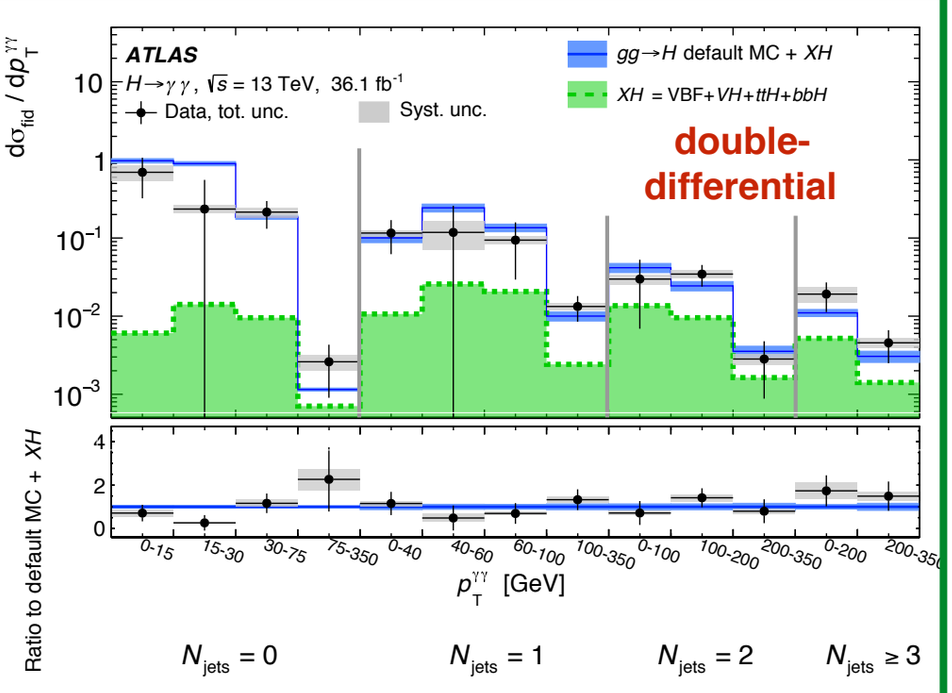

Inclusive fiducial xsec:

$$\sigma_{fid,comb} = 55 \pm 9(stat) \pm 4(\exp) \pm 0.1(theo)\, fb$$

$$\sigma_{fid,SM} = 64 \pm 2\, fb$$

~18% precision

Overall good theoretical description of data. Precision statistically limited

Total Higgs boson cross-section: H4l, Hγγ combination

ATLAS-CONF-2017-047

- Combining H→4ℓ and H→γγ measurements to improve precision on Higgs boson cross-section(*)
- Combination is done in total phase space
  - more model-dependent

$$\sigma_i = \frac{N_i^{sig}}{L B_F A_i C_i}$$

Acceptance correction

fiducial total phase space from MC:

A(H→γγ) ~ 50%, A(H→4l) ~ 42%

- assumed **SM branching fractions**: B_F(H→γγ) = 0.23% , B_F(H→ZZ*→4ℓ) = 0.013%

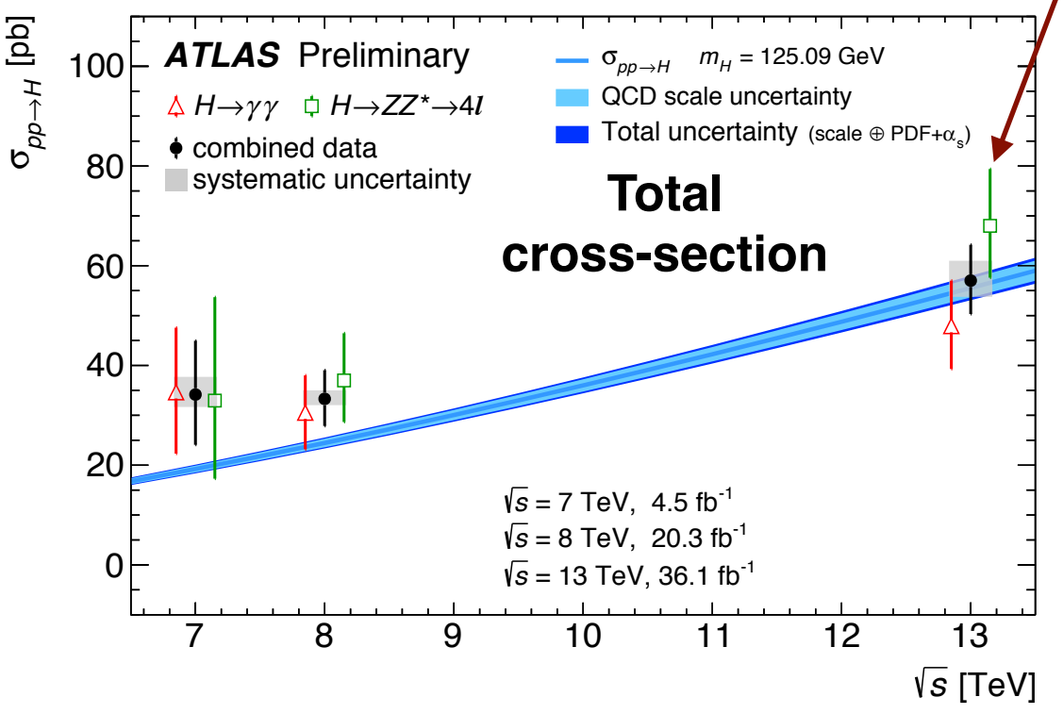

Single signal strength fit for all the production and decay modes

$$\mu = \frac{\sigma \times B}{(\sigma \times B)_{SM}}$$

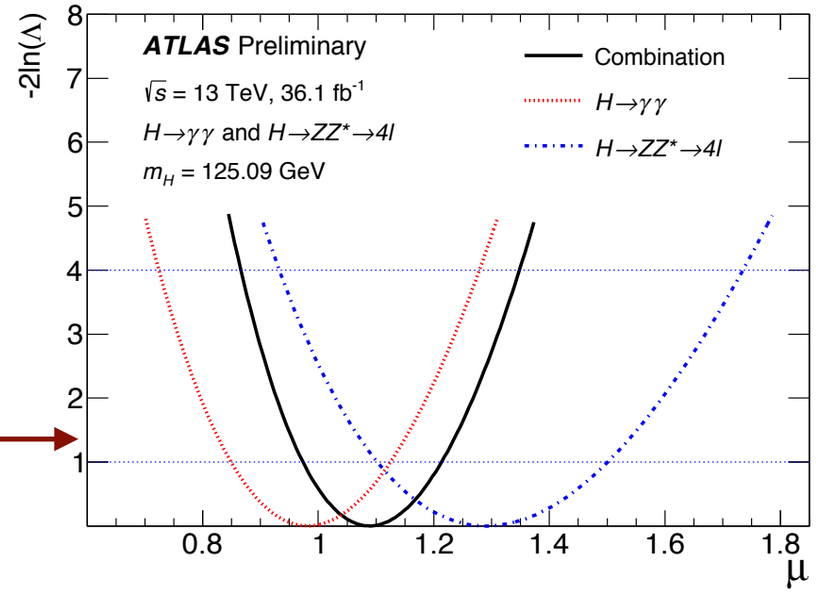

$$\mu = 1.09 \pm 0.09(stat.)^{+0.06}_{-0.05}(\exp.)^{+0.06}_{-0.05}(th.)$$

Combined measurement in agreement with SM prediction

Decay channel	Total cross section ($pp \to H + X$) $\sqrt{s}$ =7 TeV	$\sqrt{s}$ =8 TeV	$\sqrt{s}$ =13 TeV
$H \to \gamma\gamma$	35^{+13}_{-12} pb	$30.5^{+7.5}_{-7.4}$ pb	$47.9^{+9.1}_{-8.6}$ pb
$H \to ZZ^* \to 4\ell$	33^{+21}_{-16} pb	37^{+9}_{-8} pb	$68.0^{+11.4}_{-10.4}$ pb
Combination	34 ± 10 (stat.) $^{+4}_{-2}$ (syst.) pb	$33.3^{+5.5}_{-5.3}$ (stat.) $^{+1.7}_{-1.3}$ (syst.) pb	$57.0^{+6.0}_{-5.9}$ (stat.) $^{+4.0}_{-3.3}$ (syst.) pb
SM prediction [8]	19.2 ± 0.9 pb	24.5 ± 1.1 pb	$55.6^{+2.4}_{-3.4}$ pb

(*)H→WW will be added in a later step

Total Higgs boson cross-section: H4l, H$\gamma\gamma$ combination

ATLAS-CONF-2018-002

Differential distributions: Higgs observables

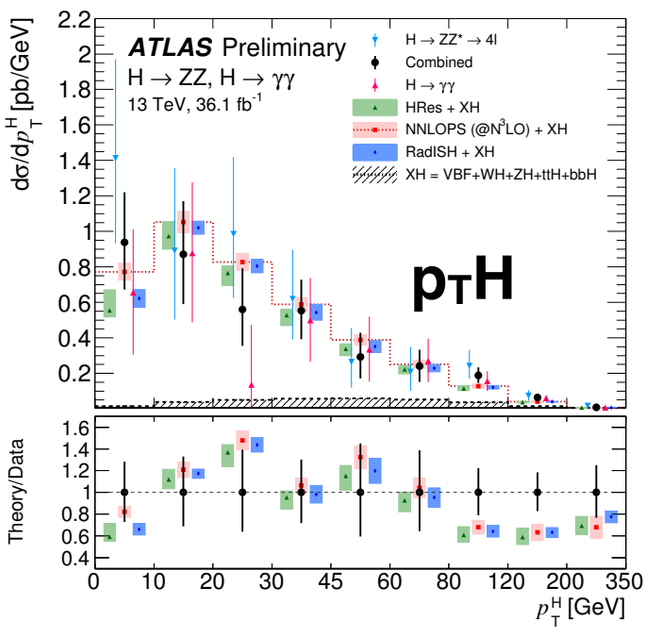

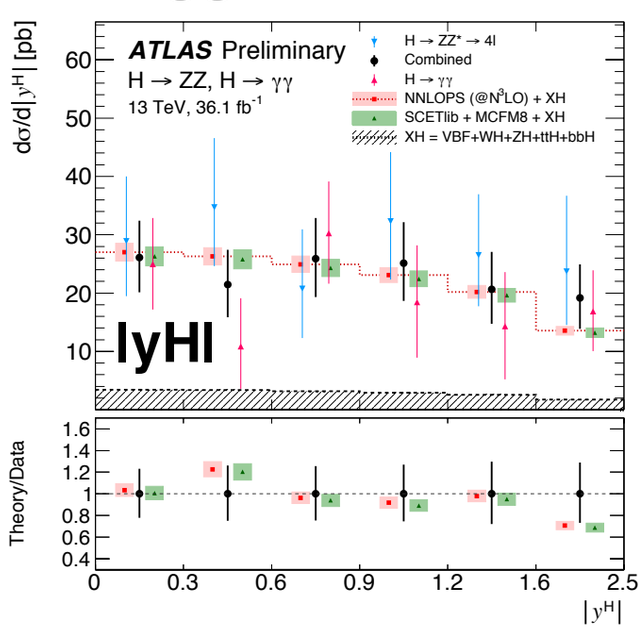

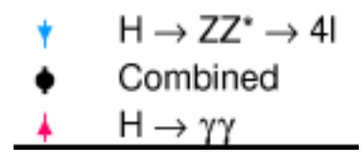

Statistical precision: 20-30% (improved combining)
Systematics uncertainties: ~10% (larger for Njets ≥ 2)

Differential distributions: Jets observables

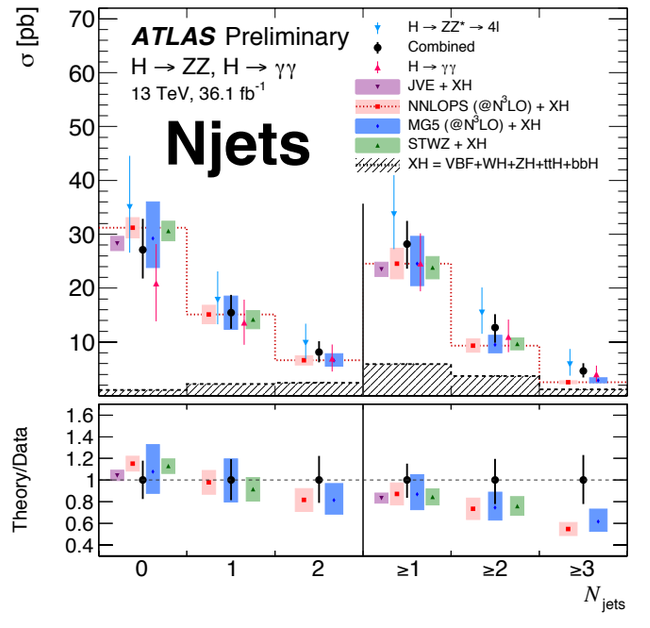

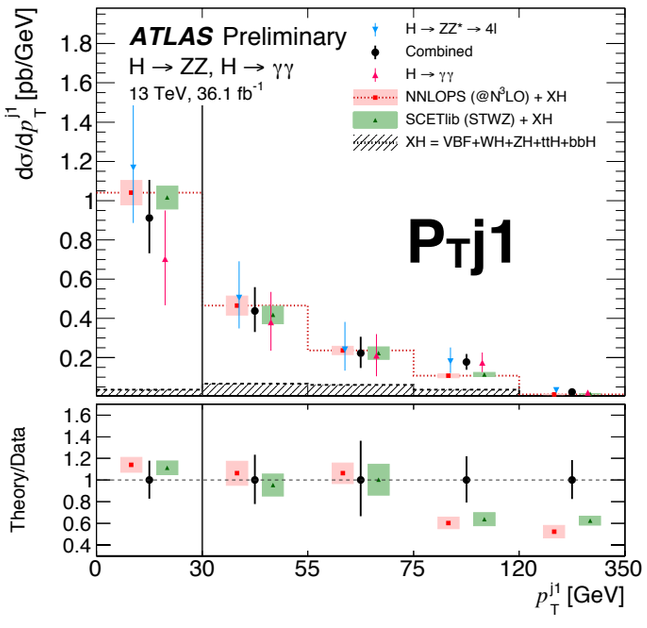

Total and differential measurements limited by statistics
More data and channels will further improve!

Single channel and combination compared with several theory predictions(*):

p-values [%]	$p_{\mathrm{T}}^{\mathrm{H}}$	$\lvert y^{\mathrm{H}}\rvert$	N_{jets}	$p_{\mathrm{T}}^{\mathrm{j1}}$
NNLOPS (@N^{3}LO)	29	92	45	5
HRes	5	–	–	–
RaDISH + NNLOJET	29	–	–	–
SCETlib	–	91	–	21
MadGraph5_aMC@NLO (@N^{3}LO)	–	–	57	–

(*)
-NNLOPS normalised to N3LO cross section, nominal sample
- HRes (NNLO+NNLL)
- RaDISH (NNLL)+NNLOJET
- SCETlib+MCMF8 (NNLO+NNLL')
- MG5_aMC@NLO (@N3LO), NLO for 0,1,2 additional jets

Production mode cross-sections in kinematic bins

1. Combined H→4l and H→γγ for |y(H)| < 2.5 in **Higgs boson production categories**: **ggF, VBF, VH and ttH**. bbH included in ggF while tHX in ttH

ATLAS-CONF-2017-047
ATLAS-CONF-2018-002

2. Provided **cross-sections and BF ratios**
   => common systematic uncertainties cancel

Quantity		Result	Uncertainty				SM prediction
			Total	Stat.	Exp.	Th.	
$\sigma_{ggF}\cdot B_{4\ell}$	[fb]	6.6	$^{+1.2}_{-1.0}$	$\left(^{+1.1}_{-1.0}\right.$	±0.4	$\left.\pm0.2\right)$	$5.6^{+0.3}_{-0.4}$
$B_{\gamma\gamma}/B_{4\ell}$		12.5	$^{+2.8}_{-2.3}$	$\left(^{+2.6}_{-2.2}\right.$	$^{+0.9}_{-0.7}$	$\left.\pm0.2\right)$	18.1 ± 0.2
$\sigma_{VBF}/\sigma_{ggF}$	$[10^{-2}]$	21.5	$^{+8.5}_{-6.3}$	$\left(^{+7.3}_{-5.6}\right.$	$^{+2.8}_{-1.7}$	$\left.^{+3.6}_{-2.2}\right)$	$7.9^{+0.4}_{-0.6}$
σ_{VH}/σ_{ggF}	$[10^{-2}]$	0.2	$^{+4.5}_{-3.4}$	$\left(^{+4.2}_{-3.2}\right.$	$^{+1.2}_{-0.9}$	$\left.^{+0.9}_{-0.4}\right)$	$4.5^{+0.2}_{-0.3}$
$\sigma_{t\bar{t}H}/\sigma_{ggF}$	$[10^{-2}]$	0.7	$^{+1.0}_{-0.9}$	$\left(^{+1.0}_{-0.9}\right.$	$^{+0.2}_{-0.1}$	$\left.\pm0.1\right)$	1.3 ± 0.1

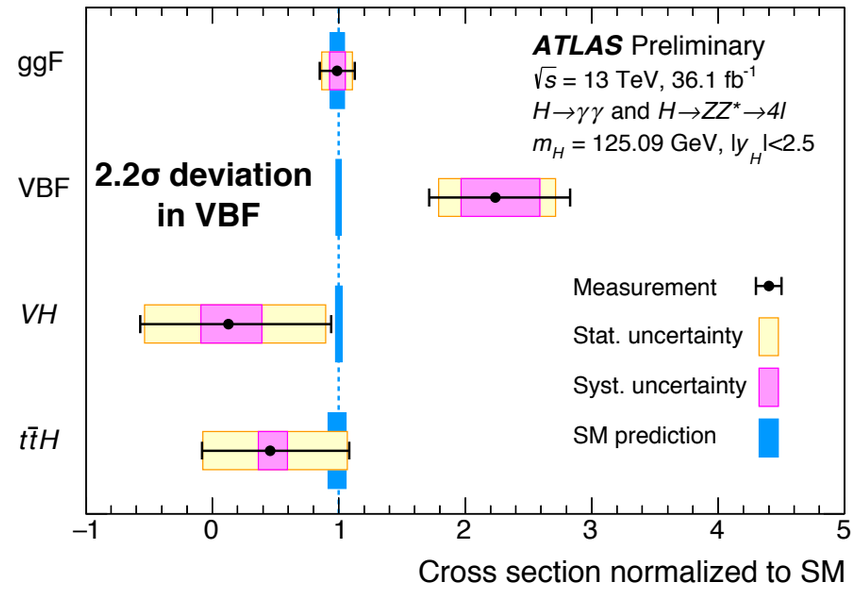

Best precision in ggF(14%) and VBF(26%)

3. Reduce model dependance by defining **exclusive kinematic regions** targeting specific production modes:
   - categories based on Higgs and associated particles kinematic (bins of Njets, $p_{TH/jet}$,..)

Best precisions ~20%

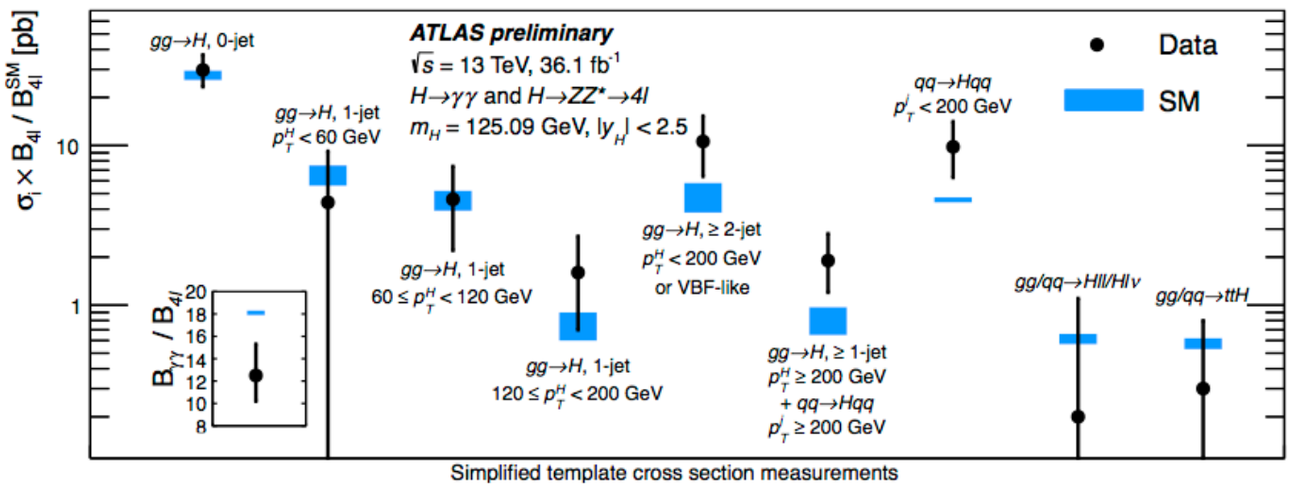

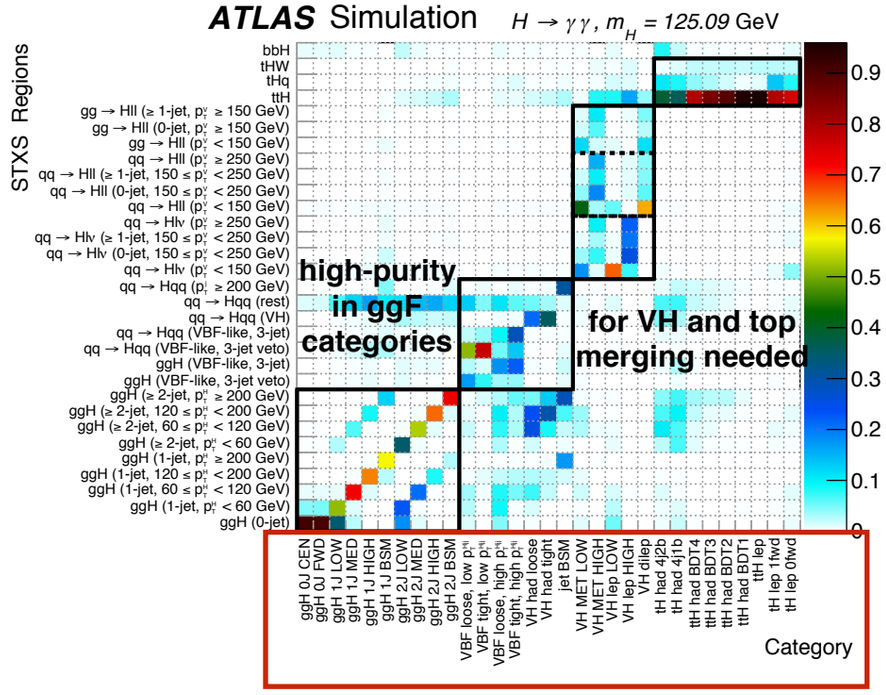

Categories in H→γγ

Higgs boson couplings measurement

ATLAS-CONF-2017-047
JHEP03(2018)095
arXiv:1802.04146

Cross-sections results can be interpreted in the contest of the couplings framework:

$$\sigma_i \cdot B^f = \frac{\sigma_i(\vec{k}) \cdot \Gamma^f(\vec{k})}{\Gamma_H}$$

couplings modifiers

example in ggF mode

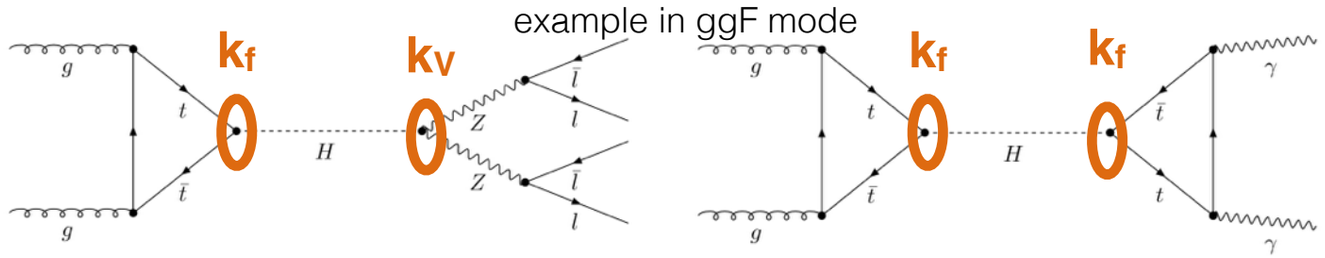

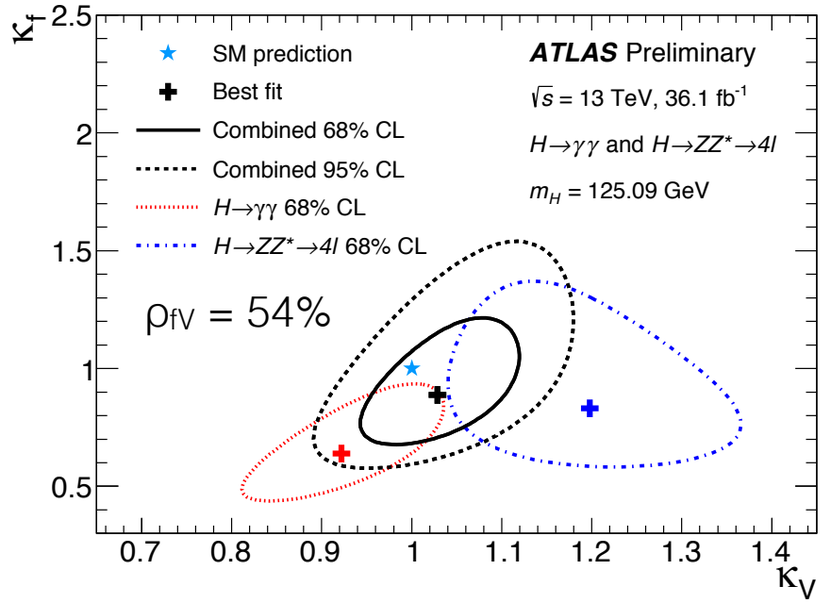

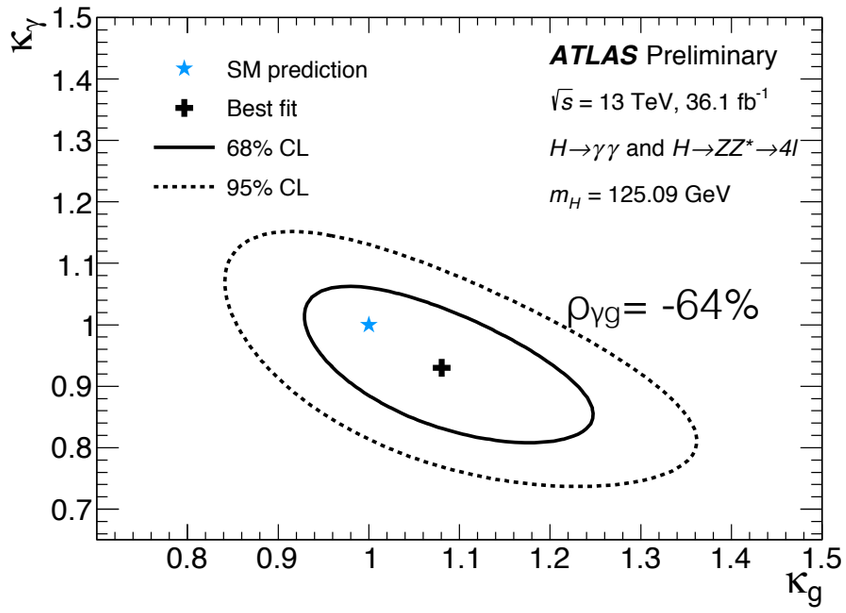

Coupling modifiers
to vector bosons and fermions (k_V, k_f)
or to loop contributions (k_g, k_γ)

No significant deviation from SM prediction observed

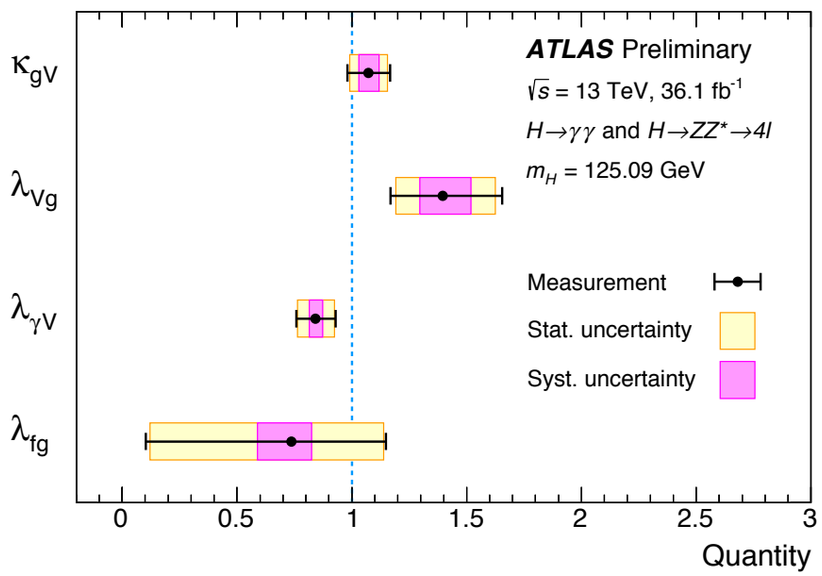

Construct ratios to probe simultaneously k_V, k_f, k_g, k_γ and the Higgs boson width Γ_H

$k_{gV} = k_g k_V / k_H$, $\lambda_{Vg} = k_V / K_g$,

$\lambda_{\gamma V} = k_\gamma / k_V$, $\lambda_{fg} = k_f / k_g$

Higgs boson mass measurement

ATLAS-CONF-2017-046

- Higgs boson mass measured in H→ZZ*→4ℓ/H→γγ channels, profiting from the fully reconstructed narrow peak over a smooth background:
  - **H→4ℓ** per-event measurement with fit in BDT bins to further distinguish signal against ZZ*. **Statistically limited** channel
  - **H→γγ** fit to $m_{\gamma\gamma}$ distribution modelled with a double-sided Crystal-ball function
  - Same categories as in cross-section measurement
  - Channel **dominated by systematic uncertainty** on photon energy scale

H_{4l} mass variation per channel

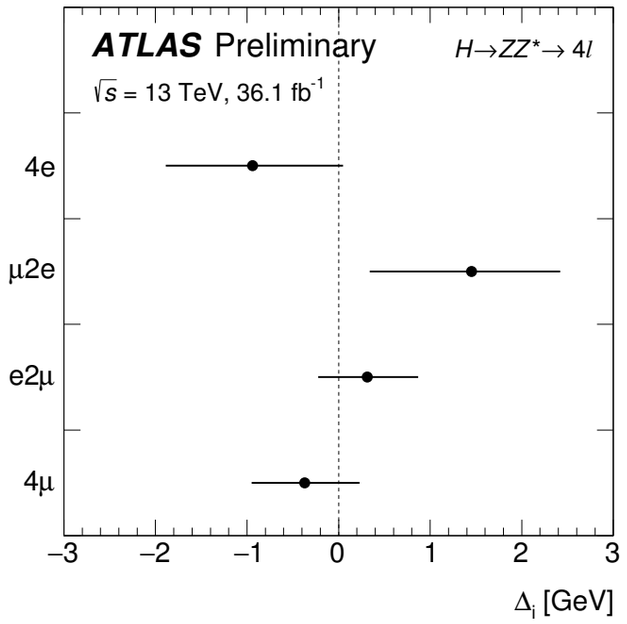

$H_{\gamma\gamma}$ mass variation for different categories (barrel/endcap or converted/uncoverted)

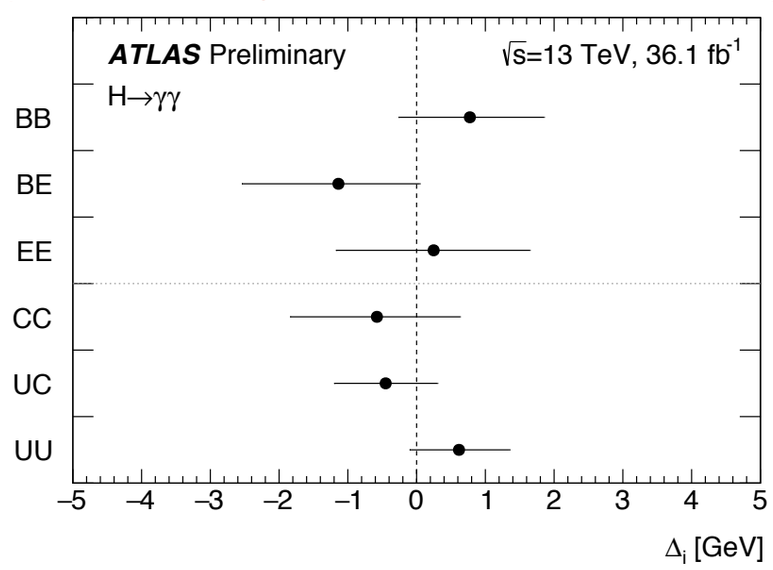

Combined mass result

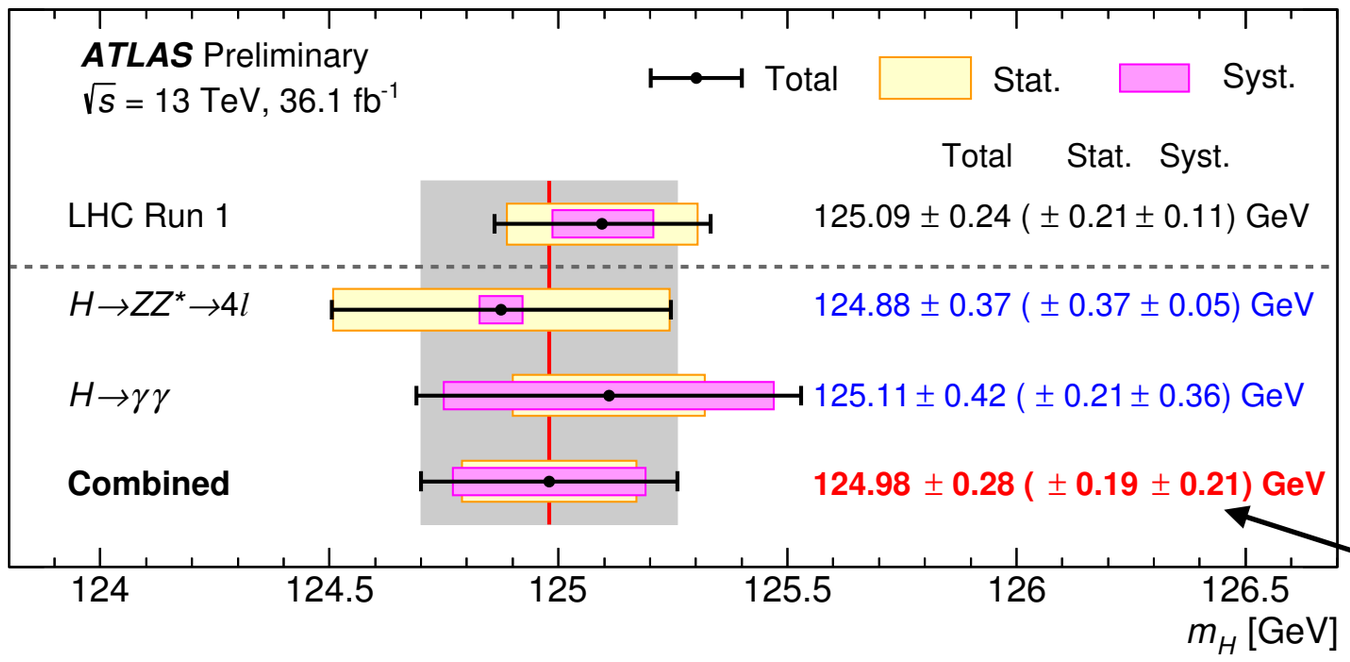

In agreement and with a similar precision to the ATLAS+CMS Run-I combination: m_H = 125.09 ± 0.24 GeV

Other Higgs boson properties

Width

Eur. Phys. J. C (2015) 75:335

- SM predicts Γ_H ~ 4 MeV → too low to be measured at LHC (resolution ~1-2 GeV)
- **Indirect constraint on Γ_H by studying off-shell Higgs boson production** in diboson final states:
  - when $m_{VV} >> m_H$, the cross-section doesn't depend on Γ_H
  - by assuming same on-shell and off-shell couplings:

$$\mu_{off-shell} = \mu_{on-shell} \cdot \Gamma_H / \Gamma_{H,SM}$$

$\Gamma_H < 22.7$ MeV @ 95%CL (<33 MeV exp.)

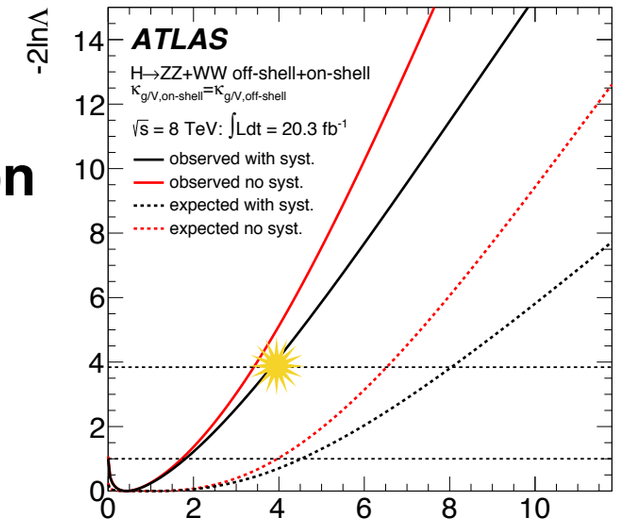

Run-I WW*/ZZ* 20.3 fb^{-1} result

Spin/CP

Run-I: Eur. Phys. J. C75 (2015) 476
Run-II: arXiv:1802.04146, JHEP03(2018)095

- **Spin and Parity of the Higgs boson measured in WW*/ZZ* final states using Run-I 7 TeV and 8 TeV data** (~25 fb^{-1}). SM Higgs boson hypothesis, **$J^P = 0^+$**, tested against alternative spin scenarios, which were excluded at 99.9% CL.
- In Run-II **Higgs boson spin-CP tested, e.g.** in γγ decays, **with angle distributions of photons and jets** sensitive to these properties

the drop is compatible with a scalar particle

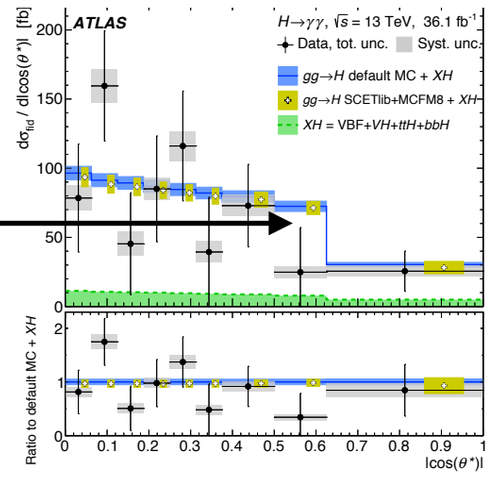

All measurements compatible with a SM Higgs boson

Remarks and Conclusions

- A summary of the first set of ATLAS Run-II Higgs boson properties measurements has been presented
  - Precision of cross-section measurements ~2 times better than with Run-I dataset
  - Overall, a remarkable good agreement with SM predictions observed

- Most of the measurements limited by statistics:
  - So far analysed ~36 fb^{-1} → ~45 fb^{-1} still in the pipeline ready to be used
  - And more data expected in the last year of LHC Run-2 data-taking

Stay tuned for the sequel
of the Higgs characterisation saga!

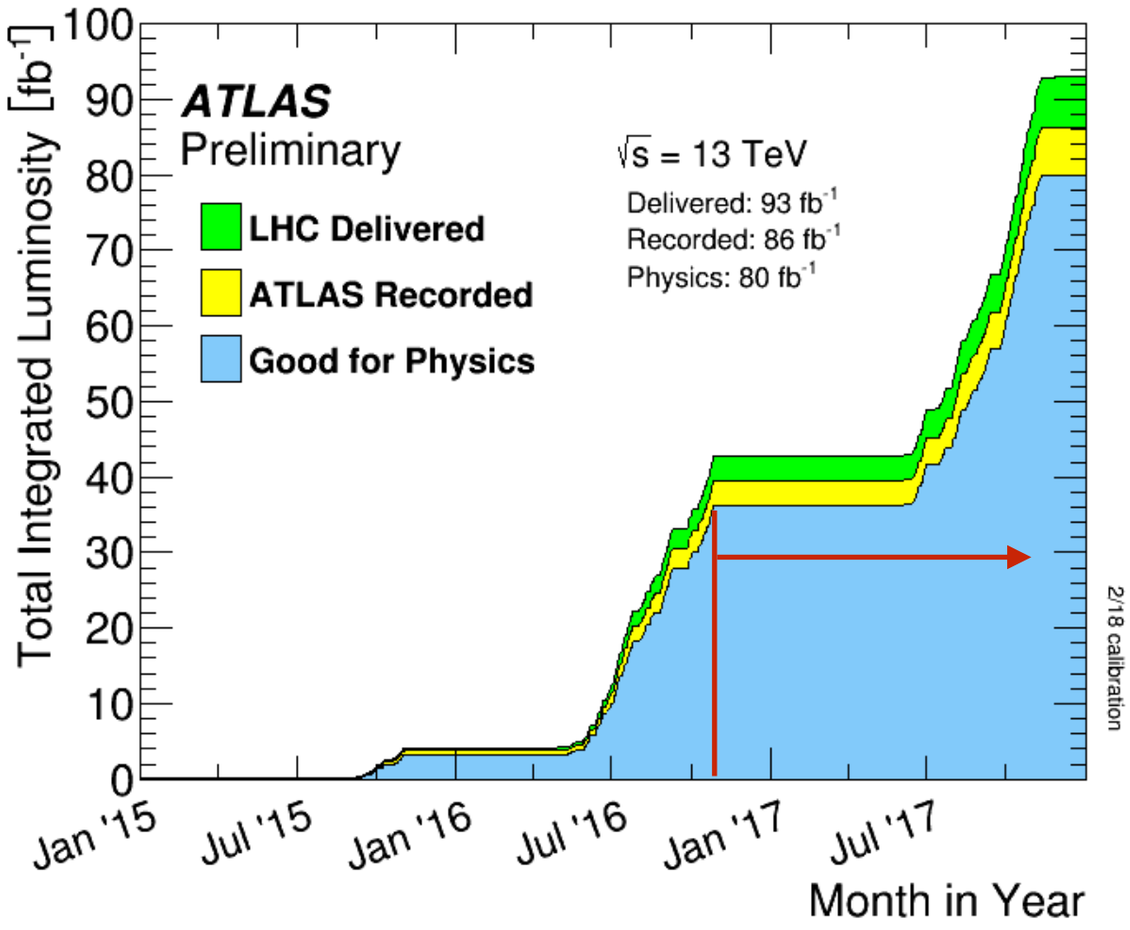

Backup

H→WW*→evμv - Analysis

ATLAS-CONF-2018-004

Analysis strategy

- **Signature**: two prompt isolated leptons and missing momentum

- **Events split in 3 Signal Regions** on Njets(*):
  - **Njet = 0 and Njet = 1 (ggF dominated)**
    - Spin 0 Higgs → leptons close together
      $\Delta\phi_{\ell\ell} < 1.8$ and $m_{\ell\ell} < 55$ GeV
    - m_T used as discriminant
  - **Njet ≥ 2 (VBF dominated)**
    - BDT used as discriminant
      - mjj and Δyjj highest ranking (2 recoiling, well-separated jets)

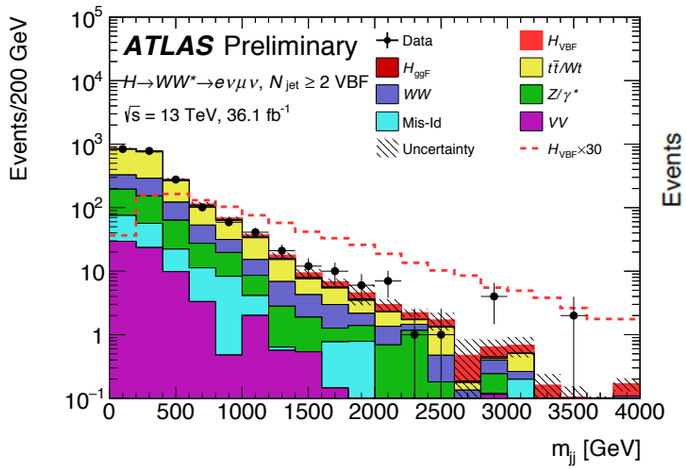

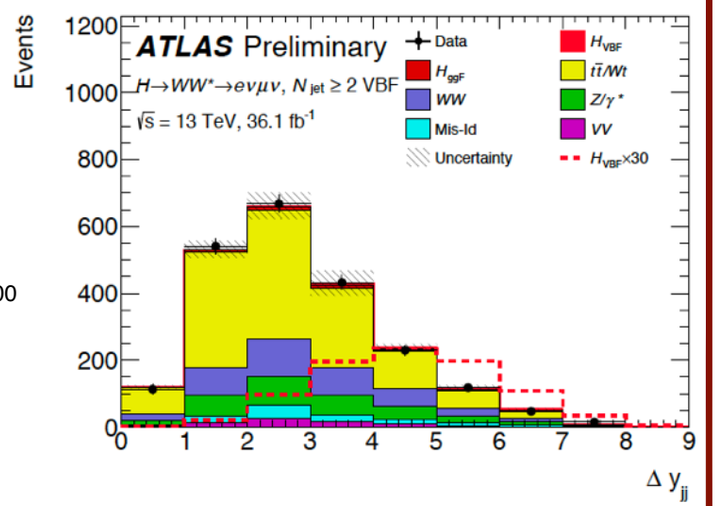

- b-jet veto in all categories to reduce ttbar ($\sigma_{13\ TeV}/\sigma_{8\ TeV} \approx 3.3$)

Backgrounds estimation

- **Irreducible background** normalised from Data control samples:
  - **non-resonant WW** (from Njets <=1 high $m_{\ell\ell}$ events)
  - **ttbar** (b-tag requirement)
  - **Z→ττ** (mττ or $\Delta\phi_{\ell\ell}$ inverted)

- **Mis-identified leptons from data** with lepton failing ID/isolation
  - large uncertainties but on a ~10% background

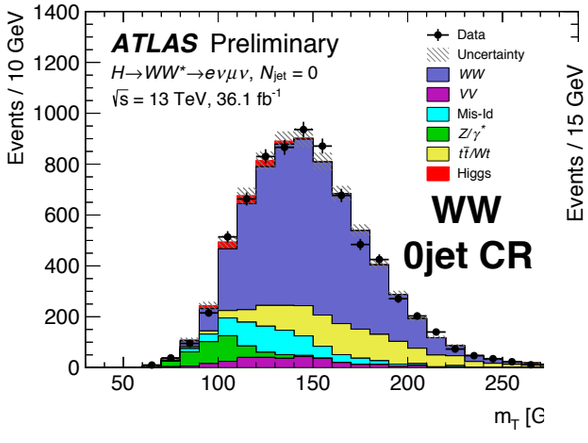

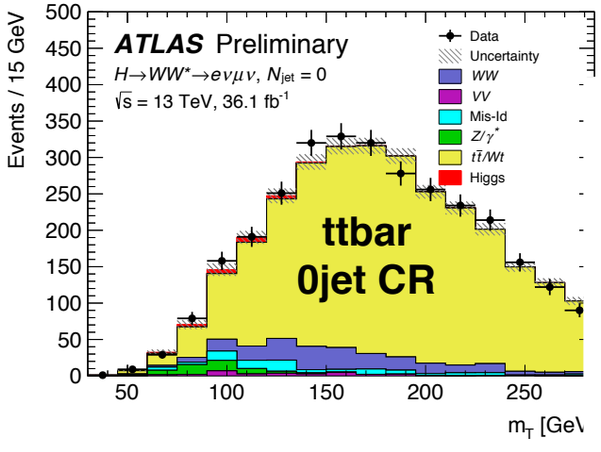

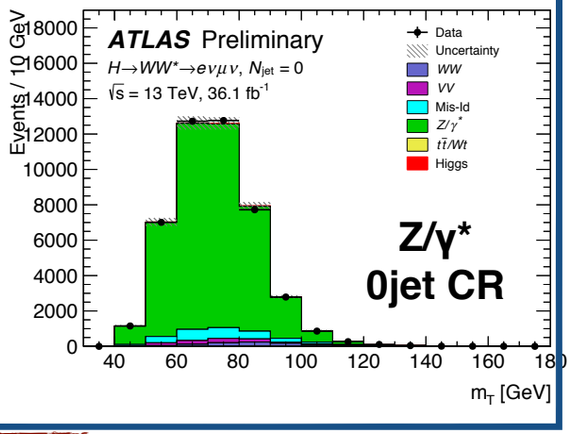

- Other minor backgrounds from simulation

(*) complete event selection table in backup

H→WW*→eνμν - Results

- Simultaneous SRs and CR max likelihood fit
  - **16 fits regions defined for Njets = 0/1**:

$$[2 \times m_{\ell\ell}] \bullet [2 \times p_T^{sub-leading}] \bullet [e\mu / \mu e]$$

- Different bkg composition
- Enhance sensitivity

  - **4 BDT bins for VBF enriched category**
    - S(VBF)/B ~0.6 in the last bin

⇒ extract both ggF and VBF cross-sections

- Other production/decays modes fixed to SM

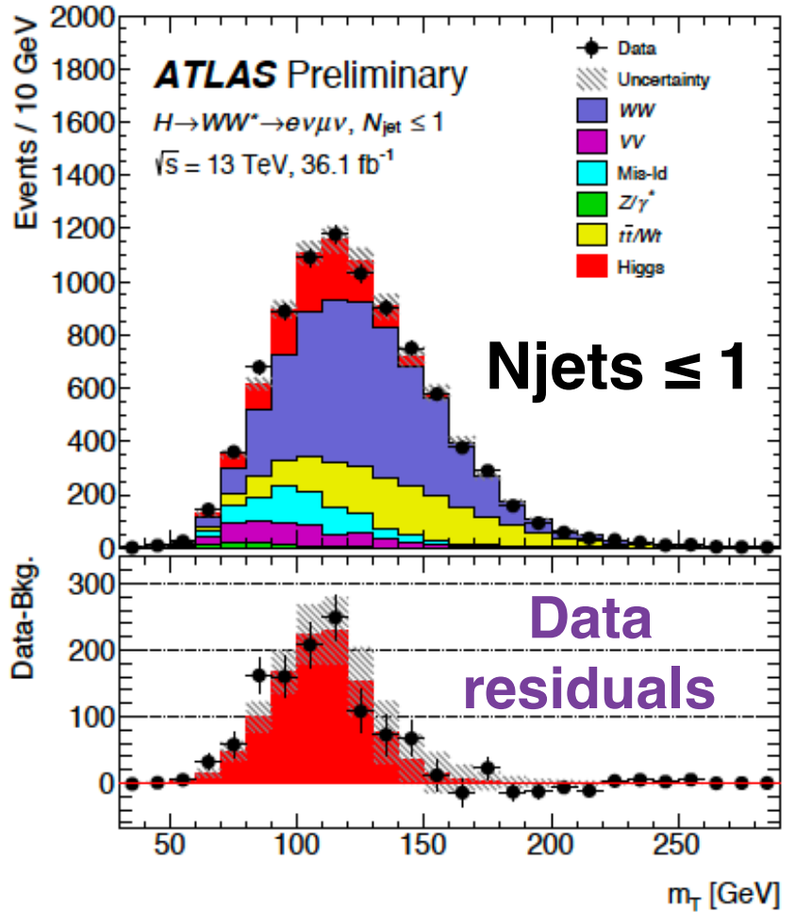

ggF: 6.3σ (exp. 5.2σ)

VBF: 1.9σ (exp. 2.7σ)

(*)

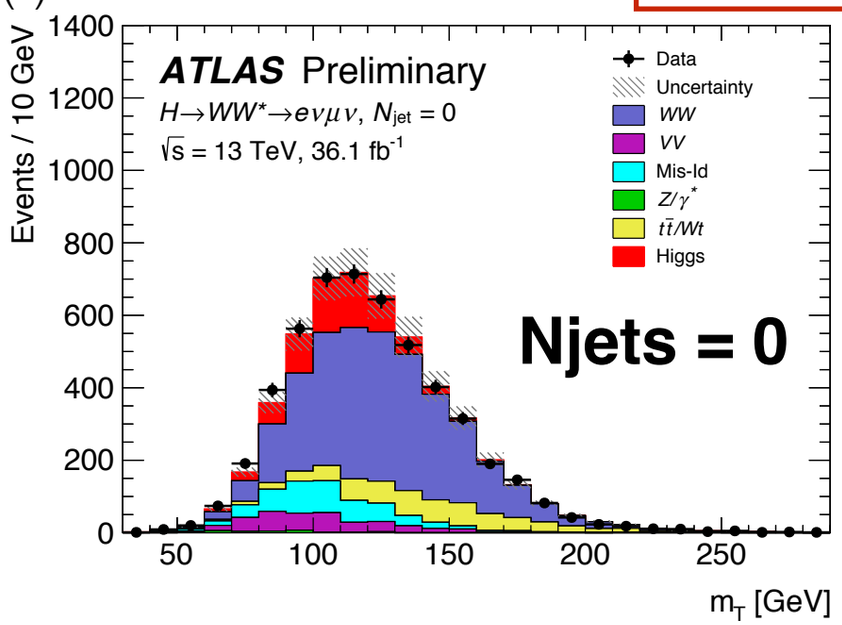

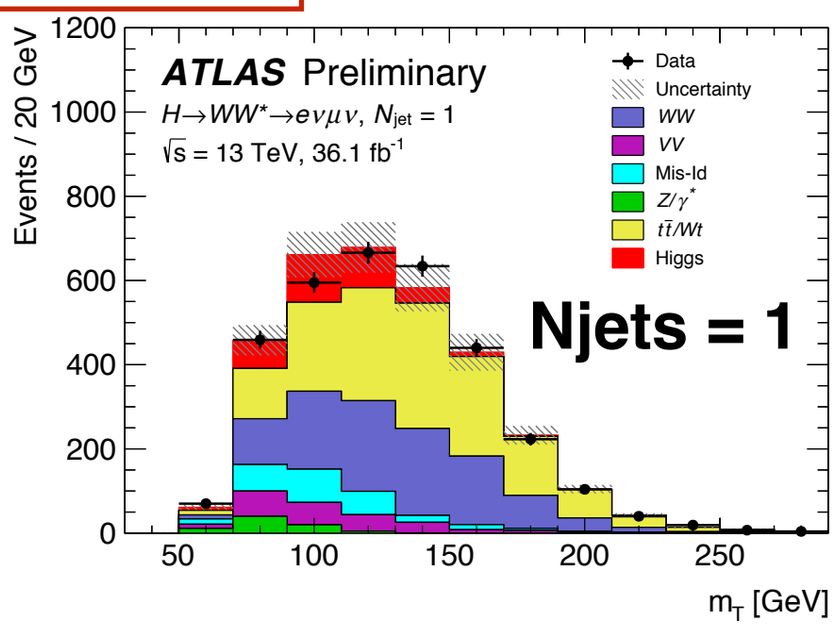

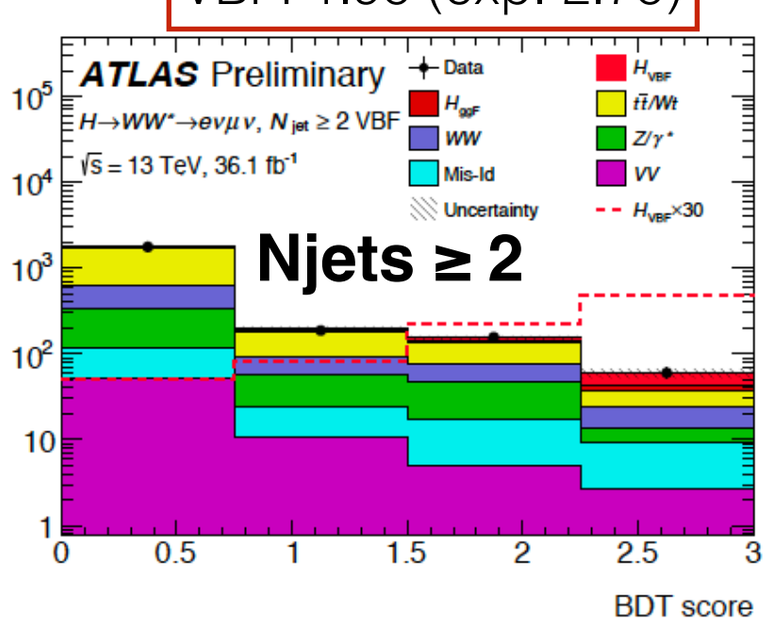

(*) all plots are post-fit

H→WW*→eνμν - Results

Signal strength and cross-section results:

	Run-2	Run-1
μ_{ggF}	$= 1.21^{+0.12}_{-0.11}(\text{stat.})^{+0.18}_{-0.17}(\text{sys.}) = 1.21^{+0.22}_{-0.21}$	$\mu_{ggF} = 1.02^{+0.29}_{-0.26}$
μ_{VBF}	$= 0.62^{+0.30}_{-0.28}(\text{stat.}) \pm 0.22(\text{sys.}) = 0.62^{+0.37}_{-0.36}$	$\mu_{VBF} = 1.27^{+0.53}_{-0.45}$

ggF: Precision improved by 36%
VBF: Limited due higher pile-up ⇒ higher bkg

$$\sigma_{\text{ggF}} \cdot \mathcal{B}_{H\to WW^*} = 12.6^{+1.3}_{-1.2}(\text{stat.})^{+1.9}_{-1.8}(\text{sys.})\ \text{pb} = 12.6^{+2.3}_{-2.1}\ \text{pb}$$
$$\sigma_{\text{VBF}} \cdot \mathcal{B}_{H\to WW^*} = 0.50^{+0.24}_{-0.23}(\text{stat.}) \pm 0.18(\text{sys.})\ \text{pb} = 0.50^{+0.30}_{-0.29}\ \text{pb}.$$

68% and 95% CL contours

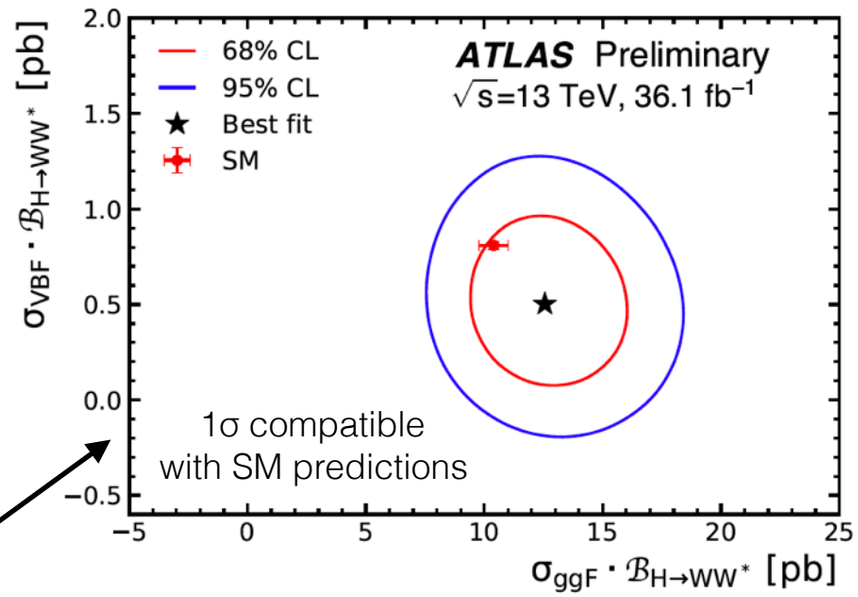

Uncertainties on the cross-sections measurement:

Source	$\frac{\Delta\sigma_{\text{ggF}}}{\sigma_{\text{ggF}}}$ [%]	$\frac{\Delta\sigma_{\text{VBF}}}{\sigma_{\text{VBF}}}$ [%]
Data statistics	±8	±46
CR statistics	±8	±9
MC statistics	±5	±23
Theoretical uncertainties	±8	±21
ggF signal	±5	±15
VBF signal	<1	±15
WW	±5	±12
Top-quark	±4	±4
Experimental uncertainties	±9	±8
b-tagging	±5	±6
Pile-up	±5	±2
Jet	±3	±4
Electron	±3	<1
Misidentified leptons	±5	±9
Luminosity	±2	±3
TOTAL	±17	±59

Significant uncertainties from Theory:
- ~5% on $\sigma_{(ggF)}$ due to WW background modelling
- 15% on $\sigma_{(VBF)}$ due to QCD scale on ggF in VBF phase space

Limited MC statistics important especially **in VBF**
$\sigma_{(ggF)}$ dominated by systematics (exp~theo)

Systematic uncertainties on WW*→evμv result

Source	$\frac{\Delta\sigma_{\text{ggF}}}{\sigma_{\text{ggF}}}$ [%]	$\frac{\Delta\sigma_{\text{VBF}}}{\sigma_{\text{VBF}}}$ [%]
Data statistics	±8	±46
CR statistics	±8	±9
MC statistics	±5	±23
Theoretical uncertainties	±8	±21
ggF signal	±5	±15
VBF signal	<1	±15
WW	±5	±12
Top-quark	±4	±4
Experimental uncertainties	±9	±8
b-tagging	±5	±6
Pile-up	±5	±2
Jet	±3	±4
Electron	±3	<1
Misidentified leptons	±5	±9
Luminosity	±2	±3
TOTAL	±17	±59

Run1/Run2 comparison for WW*→evμv result

	μ_{ggF}	stat.	syst.
ATLAS, 13 TeV, 36.1 fb^{-1}	$1.21^{+0.22}_{-0.21}$	10%	15%
ATLAS, 7+8 TeV, 24.8 fb^{-1}	$1.02^{+0.29}_{-0.26}$	19%	20%
CMS, 13 TeV, 35.9 fb^{-1}	$1.38^{+0.21}_{-0.24}$	-	-

	μ_{VBF}	total
ATLAS, 13 TeV, 36.1 fb^{-1}	$0.62^{+0.37}_{-0.36}$	59%
ATLAS, 7+8 TeV, 24.8 fb^{-1}	$1.27^{+0.53}_{-0.45}$	$^{+41\%}_{-35\%}$
CMS, 13 TeV, 35.9 fb^{-1}	$0.29^{+0.66}_{-0.29}$	$^{+228\%}_{-100\%}$

CMS also gives results for VH.

Theory ggF cross section prediction improved in Run 2 w.r.t. Run 1.
μ of Run 2 uses different cross section prediction than in Run 1.

- Good compatibility between Run 1 and Run 2, as well as ATLAS and CMS
- ggF: Precision improved by 36% with respect to Run 1.
  - Systematic uncertainties reduced by 25%.
- VBF signal strength low in Run 2
  - Expected significance is 2.7σ for the Run 1 and the Run 2 measurements

→ New measurements in $H \to WW^*$ will contribute to combined Higgs results

H→ZZ*→4ℓ inclusive and differential cross-section

- Experimental and particle level selection as similar as possible to minimise theory uncertainties

Fiducial phase space definition

Leptons and jets	
Muons:	$p_{\mathrm{T}} > 5$ GeV, $\lvert\eta\rvert < 2.7$
Electrons:	$p_{\mathrm{T}} > 7$ GeV, $\lvert\eta\rvert < 2.47$
Jets:	$p_{\mathrm{T}} > 30$ GeV, $\lvert y\rvert < 4.4$
Jet-lepton overlap removal:	$\Delta R(\mathrm{jet}, \ell) > 0.1\,(0.2)$ for muons (electrons)
Lepton selection and pairing	
Lepton kinematics:	$p_{\mathrm{T}} > 20, 15, 10$ GeV
Leading pair (m_{12}):	SFOS lepton pair with smallest $\lvert m_Z - m_{\ell\ell}\rvert$
Subleading pair (m_{34}):	remaining SFOS lepton pair with smallest $\lvert m_Z - m_{\ell\ell}\rvert$
Event selection (at most one quadruplet per channel)	
Mass requirements:	$50 < m_{12} < 106$ GeV and $12 < m_{34} < 115$ GeV
Lepton separation:	$\Delta R(\ell_i, \ell_j) > 0.1\,(0.2)$ for same- (different-) flavour leptons
J/ψ veto:	$m(\ell_i, \ell_j) > 5$ GeV for all SFOS lepton pairs
Mass window:	$115\ GeV < m_{4\ell} < 130$ GeV

Fiducial xsections
are defined at the particle level
==> correct the number of reconstructed events by
the difference in acceptance between detector-level and particle level

H→ZZ*→4ℓ inclusive and differential cross-section

SR event yields

Final state	SM Higgs	ZZ^*	$Z+\text{jets}$, $t\bar{t}$ WZ, ttV, VVV	Expected	Observed
4μ	20.1 ± 2.1	9.8 ± 0.5	1.3 ± 0.3	31.2 ± 2.2	33
$4e$	10.6 ± 1.2	4.4 ± 0.4	1.3 ± 0.2	16.3 ± 1.3	16
$2e2\mu$	14.2 ± 1.4	7.1 ± 0.4	1.0 ± 0.2	22.3 ± 1.5	32
$2\mu2e$	10.8 ± 1.2	4.6 ± 0.4	1.4 ± 0.2	16.8 ± 1.3	21
Total	56 ± 6	25.9 ± 1.5	5.0 ± 0.6	87 ± 6	102

Exclusive, Inclusive and Total cross-section

Cross section	Data ($\pm$ (stat) $\pm$ (sys))	LHCXSWG prediction	p-value [%]
$\sigma_{4\mu}$ [fb]	$0.92\ ^{+0.25}_{-0.23}\ ^{+0.07}_{-0.05}$	0.880 ± 0.039	88
σ_{4e} [fb]	$0.67\ ^{+0.28}_{-0.23}\ ^{+0.08}_{-0.06}$	0.688 ± 0.031	96
$\sigma_{2\mu2e}$ [fb]	$0.84\ ^{+0.28}_{-0.24}\ ^{+0.09}_{-0.06}$	0.625 ± 0.028	39
$\sigma_{2e2\mu}$ [fb]	$1.18\ ^{+0.30}_{-0.26}\ ^{+0.07}_{-0.05}$	0.717 ± 0.032	7
$\sigma_{4\mu+4e}$ [fb]	$1.59\ ^{+0.37}_{-0.33}\ ^{+0.12}_{-0.10}$	1.57 ± 0.07	65
$\sigma_{2\mu2e+2e2\mu}$ [fb]	$2.02\ ^{+0.40}_{-0.36}\ ^{+0.14}_{-0.11}$	1.34 ± 0.06	6
σ_{sum} [fb]	$3.61\ ^{+0.54}_{-0.50}\ ^{+0.26}_{-0.21}$	2.91 ± 0.13	19
σ_{comb} [fb]	$3.62\ ^{+0.53}_{-0.50}\ ^{+0.25}_{-0.20}$	2.91 ± 0.13	18
σ_{tot} [pb]	$69\ ^{+10}_{-9}\ \pm 5$	55.6 ± 2.5	19

Higgs boson signal xsections normalised at LHCXS WG predictions:

- for ggF, N3LO in QCD and NLO EW corrections applied
- VBF is fully NLO (approximate NNLO QCD corrections
- applied)

Uncertainties breakdown

Observable	Stat unc. [%]	Systematic unc. [%]	Dominant systematic components [%] e	jets	μ	ZZ^* theo	Model	$Z+\text{jets}+t\bar{t}$	Lumi
σ_{comb}	14	7	3	< 0.5	3	2	0.8	0.8	4
$\mathrm{d}\sigma/\mathrm{d}p_{\mathrm{T},4\ell}$	30 – 150	3 – 11	1 – 4	< 0.5	1 – 3	0 – 7	0 – 6	1 – 6	3 – 5
$\partial\sigma/\partial p_{\mathrm{T},4\ell}$ (0j)	31 – 52	10– 18	2 – 5	3 – 16	1 – 4	3 – 8	1	2 – 3	3 – 5
$\partial\sigma/\partial p_{\mathrm{T},4\ell}$ (1j)	35 – 15	6 – 30	1 – 4	2 – 29	1 – 3	1 – 4	1 – 11	1 – 2	3 – 5
$\partial\sigma/\partial p_{\mathrm{T},4\ell}$ (2j)	30 – 41	5 – 21	1 – 3	2 – 19	1 – 3	1 – 5	1 – 7	1 – 2	3 – 5
$\mathrm{d}\sigma/\mathrm{d}\lvert y_{4\ell}\rvert$	29 – 120	5 – 8	2 – 4	< 0.5	2 – 3	1 – 2	0 – 1	1 – 1	3 – 5
$\mathrm{d}\sigma/\mathrm{d}\lvert\cos\theta^*\rvert$	31 – 100	5 – 8	2 – 4	< 0.5	2 – 3	1 – 2	0 – 2	1 – 4	3 – 5
$\mathrm{d}\sigma/\mathrm{d}m_{34}$	26 – 53	4 – 13	2 – 5	< 0.5	1 – 5	1 – 6	0 – 1	1 – 3	3 – 5
$\partial^2\sigma/\ \partial m_{12}\ \partial m_{34}$	21 – 40	4 – 12	2 – 4	< 0.5	1 – 4	1 – 6	0 – 1	1 – 4	3 – 5
$\mathrm{d}\sigma/\mathrm{d}N_{\mathrm{jets}}$	22 – 44	6 – 31	1 – 4	4 – 22	1 – 3	2 – 4	1 – 22	1 – 2	3 – 5
$\mathrm{d}\sigma/\mathrm{d}p_{\mathrm{T}}^{\mathrm{lead.jet}}$	30 – 53	5 – 18	1 – 4	3 – 16	1 – 3	2 – 3	1 – 8	1 – 2	3 – 5
$\mathrm{d}\sigma/\mathrm{d}\Delta\phi_{\mathrm{jj}}$	29 – 43	9 – 17	1 – 3	8 – 14	1 – 3	3 – 4	1 – 7	1 – 1	3 – 5
$\mathrm{d}\sigma/\mathrm{d}m_{jj}$	23 – 100	9 – 27	1 – 4	8 – 24	1 – 4	3 – 8	1 – 7	0 – 3	3 – 5

H→ZZ*→4ℓ inclusive and differential cross-section

Bin-by-bin correction factors for detector inefficiencies and reconstruction

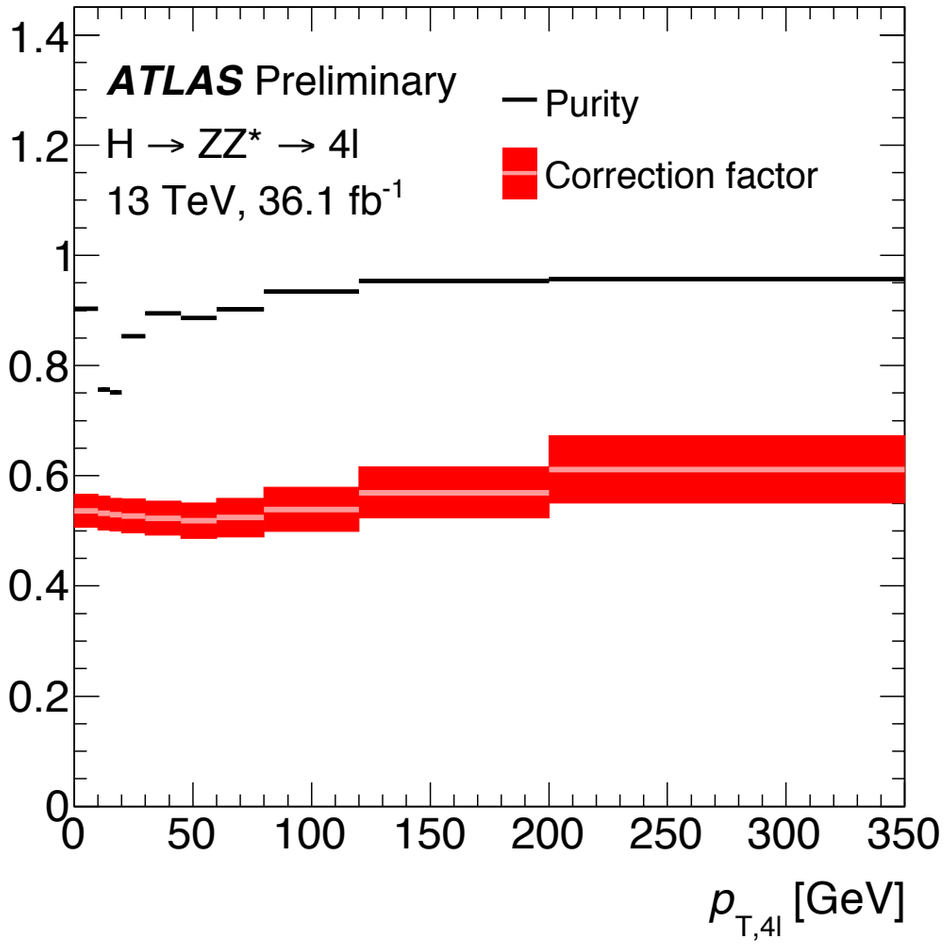

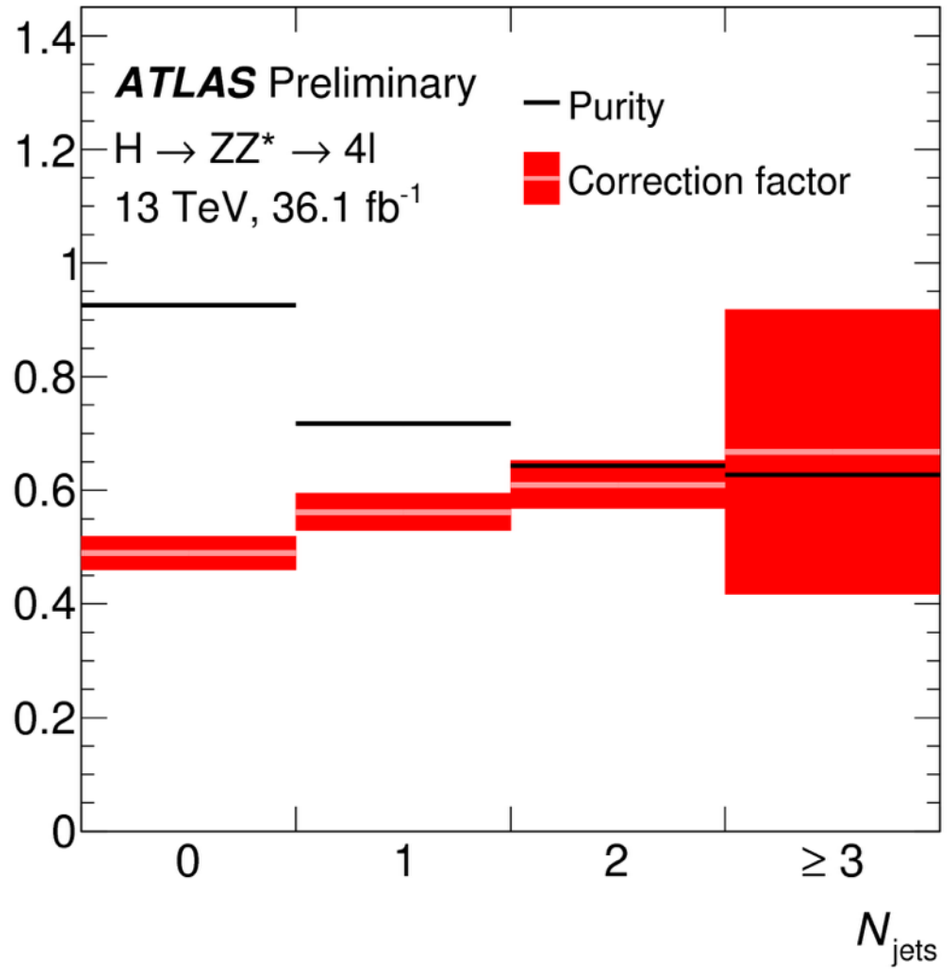

- For ggF, NNLOPS sample used to derived the correction factor
- correction factors agree within 15% for all production modes
  except for ttH, due to the missing isolation requirement needed to identify leptons from hadronic jets at particle level
- Large uncertainty on the last bin of Njets due to exp jet reconstruction uncertainty mainly

H→ZZ*→4ℓ inclusive and differential cross-section

More differential distributions…

different ggF predictions
but normalised to N3LO with the corresponding k-factors
XH processes have been added

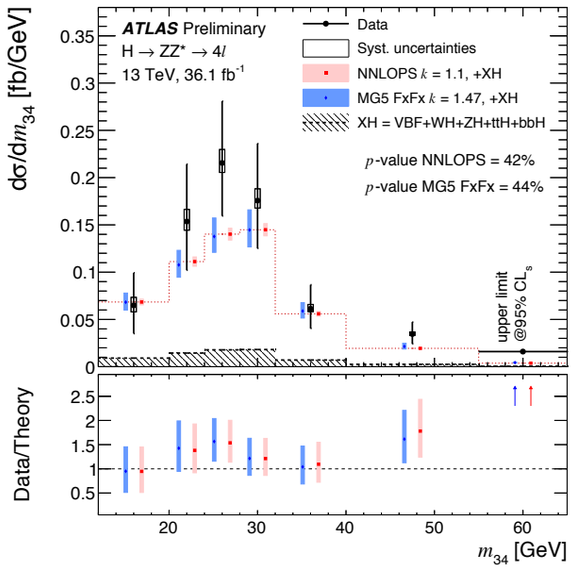

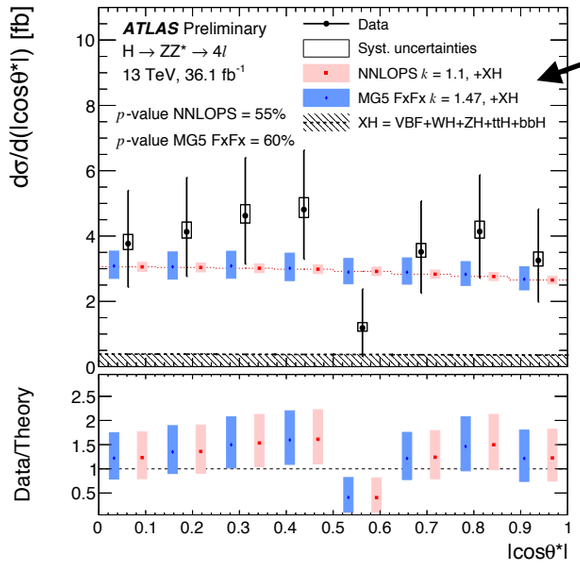

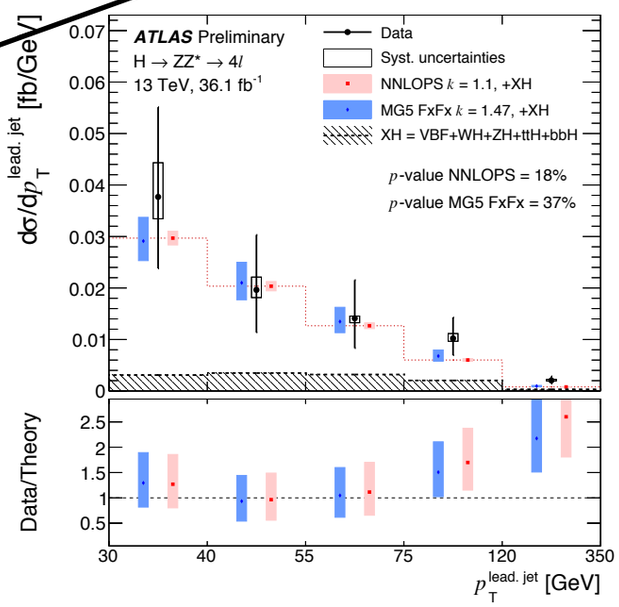

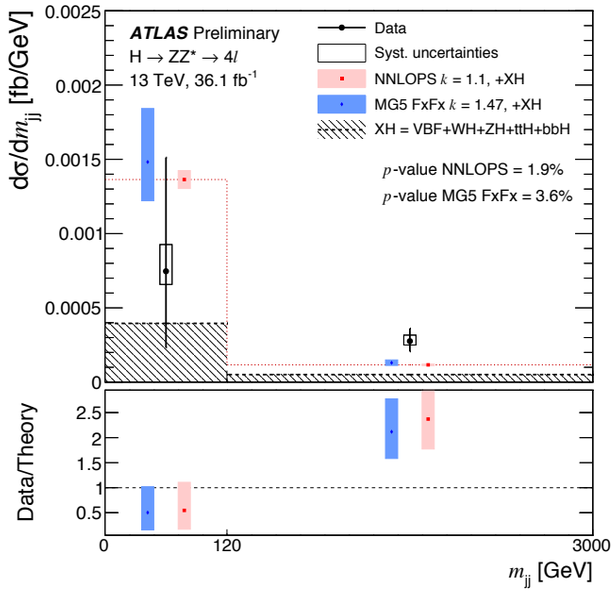

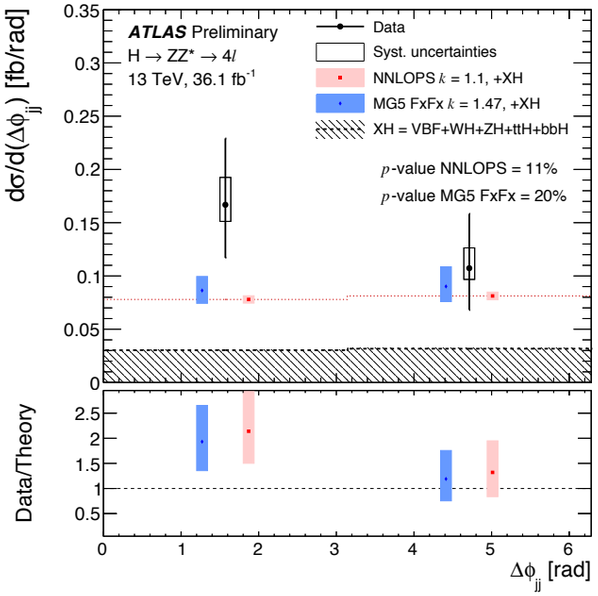

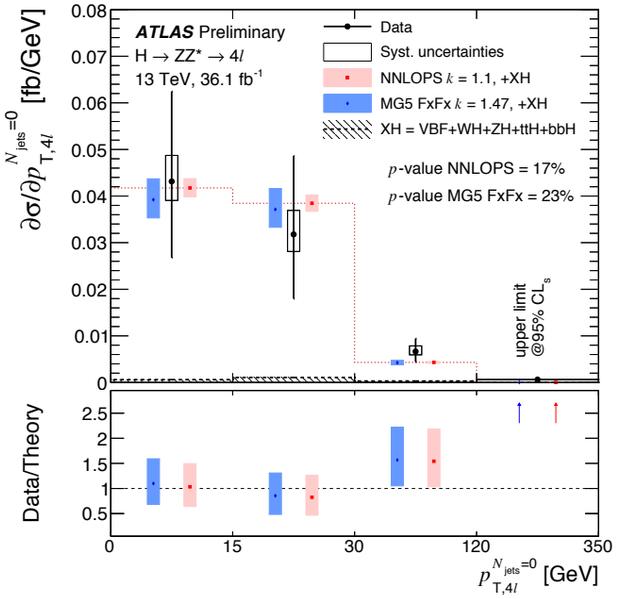

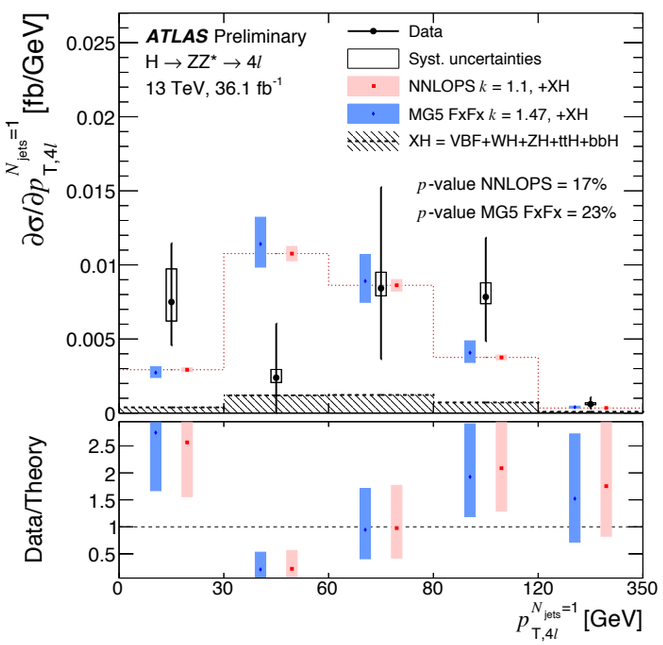

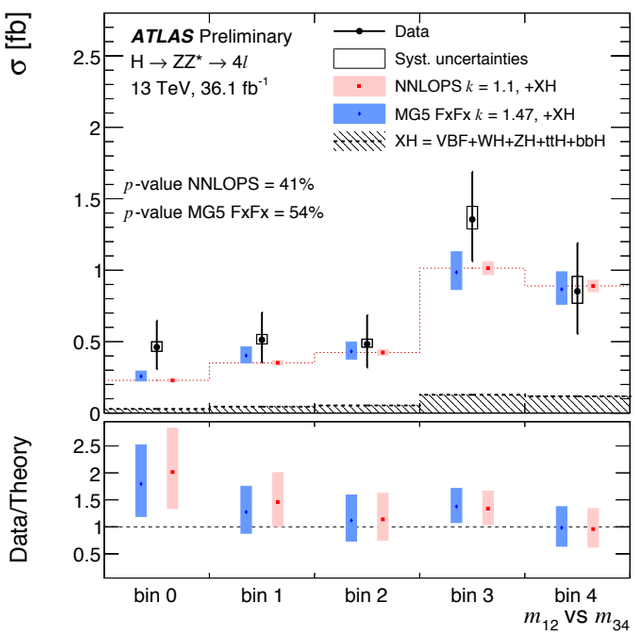

H→ZZ*→4ℓ inclusive and differential cross-section

Run-I/Run-II comparison

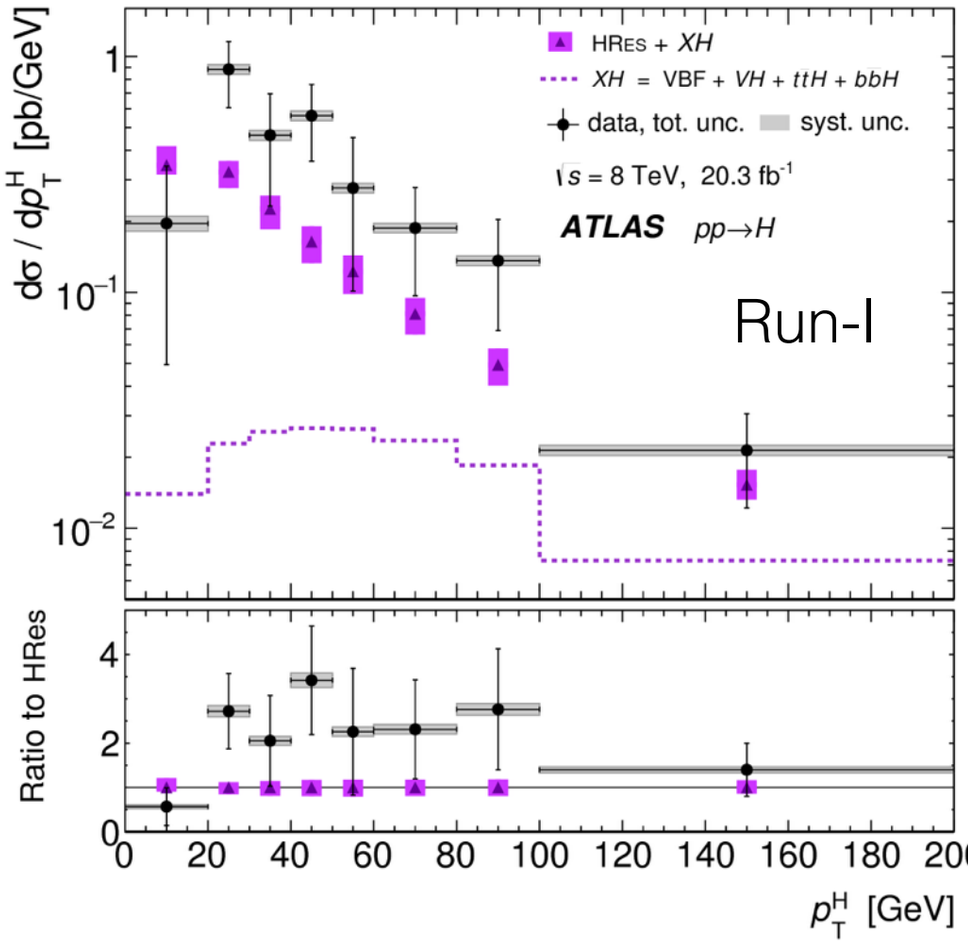

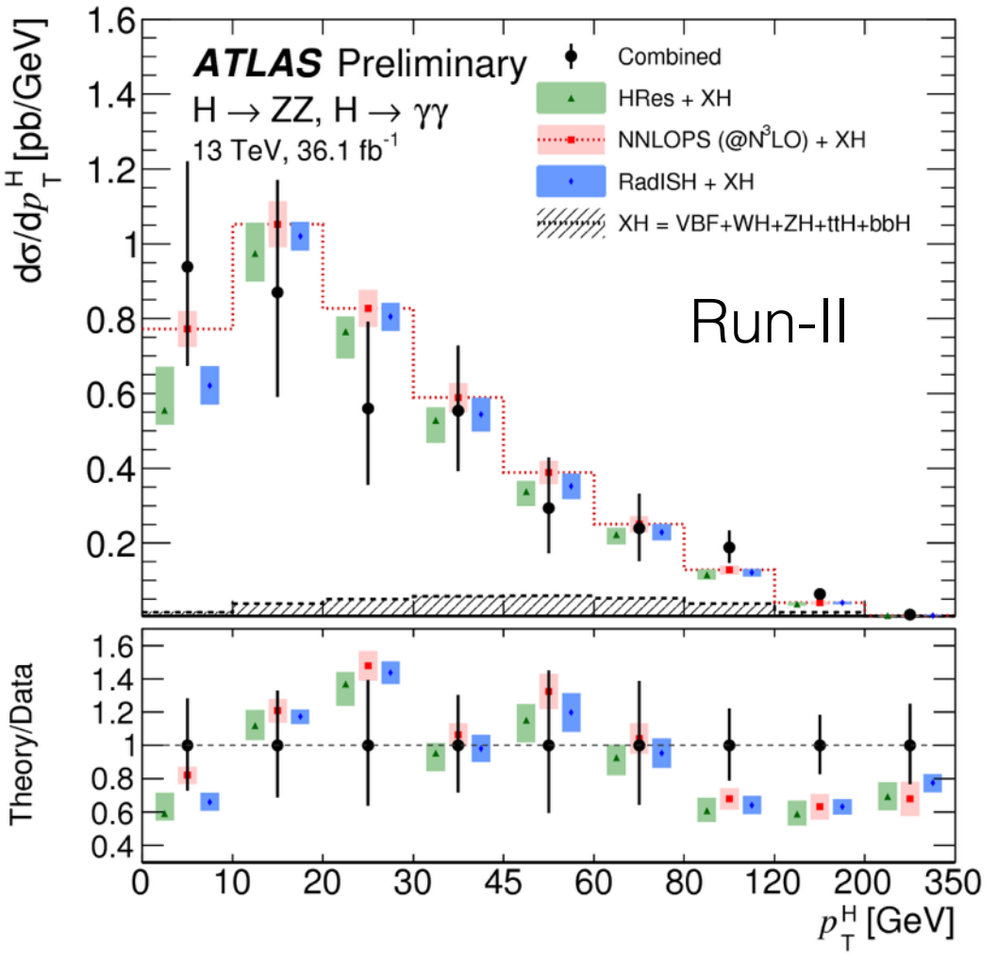

More bins at high-pt and gain in statistical precision.
Not enough sensitivity to different generators (yet)

H→γγ inclusive and differential cross-section

Table 14: Summary of the particle-level definitions of the five fiducial integrated regions described in the text. The photon isolation $p_{\mathrm{T}}^{\mathrm{iso},0.2}$ is defined analogously to the reconstructed-level track isolation as the transverse momentum of the system of charged particles within $\Delta R < 0.2$ of the photon.

Objects	Definition
Photons	$\lvert\eta\rvert < 1.37$ or $1.52 < \lvert\eta\rvert < 2.37$, $p_{\mathrm{T}}^{\mathrm{iso},0.2}/p_{\mathrm{T}}^{\gamma} < 0.05$
Jets	anti-k_t, $R = 0.4$, $p_{\mathrm{T}} > 30\,\mathrm{GeV}$, $\lvert y\rvert < 4.4$
Leptons, ℓ	e or μ, $p_{\mathrm{T}} > 15\,\mathrm{GeV}$, $\lvert\eta\rvert < 2.47$ for e (excluding $1.37 < \lvert\eta\rvert < 1.52$) and $\lvert\eta\rvert < 2.7$ for μ
Fiducial region	**Definition**
Diphoton fiducial	$N_\gamma \geq 2$, $p_{\mathrm{T}}^{\gamma_1} > 0.35\,m_{\gamma\gamma} = 43.8\,\mathrm{GeV}$, $p_{\mathrm{T}}^{\gamma_2} > 0.25\,m_{\gamma\gamma} = 31.3\,\mathrm{GeV}$
VBF-enhanced	Diphoton fiducial, $N_j \geq 2$ with $p_{\mathrm{T}}^{\mathrm{jet}} > 25\,\mathrm{GeV}$, $m_{jj} > 400\,\mathrm{GeV}$, $\lvert\Delta y_{jj}\rvert > 2.8$, $\lvert\Delta\phi_{\gamma\gamma,jj}\rvert > 2.6$
$N_{\mathrm{lepton}} \geq 1$	Diphoton fiducial, $N_\ell \geq 1$
High $E_{\mathrm{T}}^{\mathrm{miss}}$	Diphoton fiducial, $E_{\mathrm{T}}^{\mathrm{miss}} > 80\,\mathrm{GeV}$, $p_{\mathrm{T}}^{\gamma\gamma} > 80\,\mathrm{GeV}$
$t\bar{t}H$-enhanced	Diphoton fiducial, $(N_j \geq 4,\ N_{b\text{-jets}} \geq 1)$ or $(N_j \geq 3,\ N_{b\text{-jets}} \geq 1, N_\ell \geq 1)$

Measured fiducial cross-sections

Fiducial region	Measured cross section	SM prediction	
Diphoton fiducial	$55 \pm 9\,(\mathrm{stat.}) \pm 4\,(\mathrm{exp.}) \pm 0.1\,(\mathrm{theo.})\,\mathrm{fb}$	$64 \pm 2\,\mathrm{fb}$	[N^{3}LO + XH]
VBF-enhanced	$3.7 \pm 0.8\,(\mathrm{stat.}) \pm 0.5\,(\mathrm{exp.}) \pm 0.2\,(\mathrm{theo.})\,\mathrm{fb}$	$2.3 \pm 0.1\,\mathrm{fb}$	[default MC + XH]
$N_{\mathrm{lepton}} \geq 1$	$\leq 1.39\,\mathrm{fb}$ 95% CL	$0.57 \pm 0.03\,\mathrm{fb}$	[default MC + XH]
High $E_{\mathrm{T}}^{\mathrm{miss}}$	$\leq 1.00\,\mathrm{fb}$ 95% CL	$0.30 \pm 0.02\,\mathrm{fb}$	[default MC + XH]
$t\bar{t}H$-enhanced	$\leq 1.27\,\mathrm{fb}$ 95% CL	$0.55 \pm 0.06\,\mathrm{fb}$	[default MC + XH]

H→γγ inclusive and differential cross-section

More differential distributions…

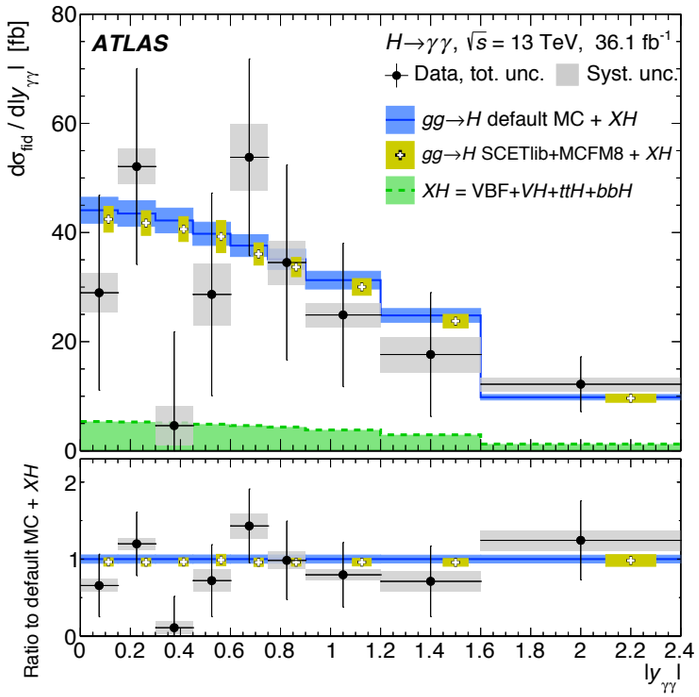

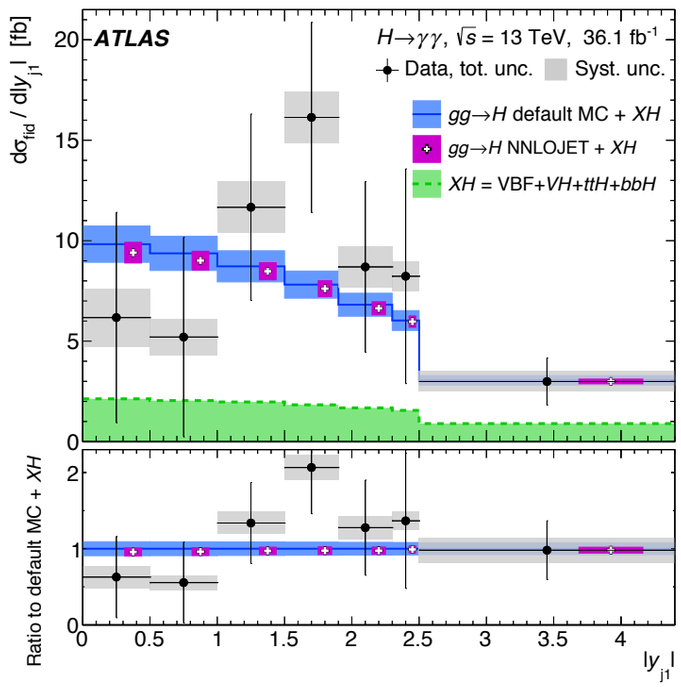

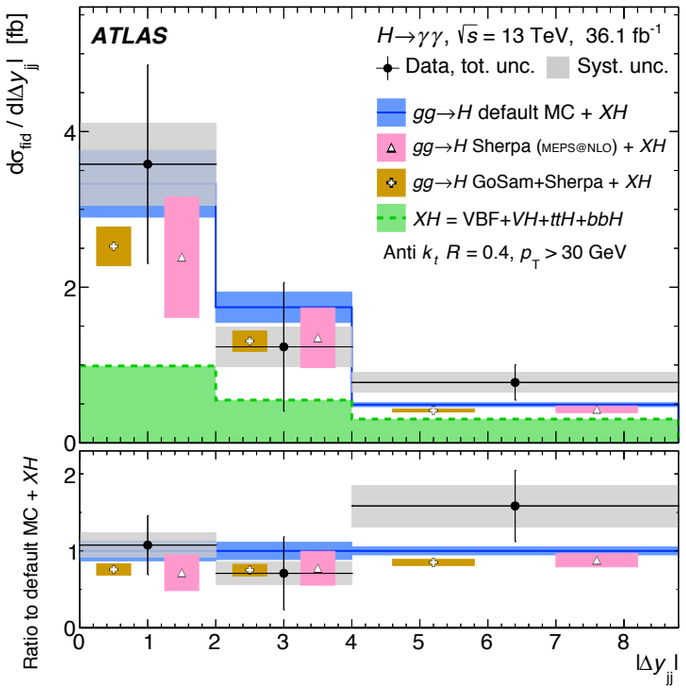

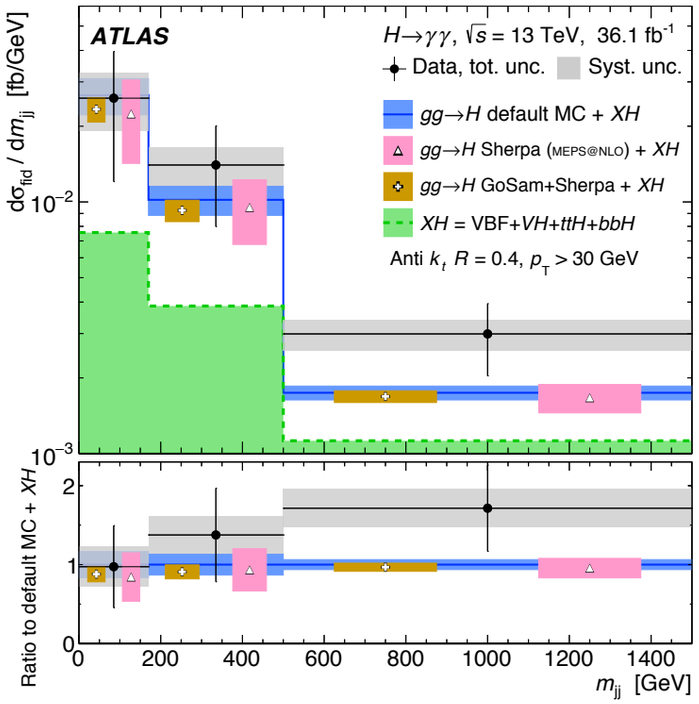

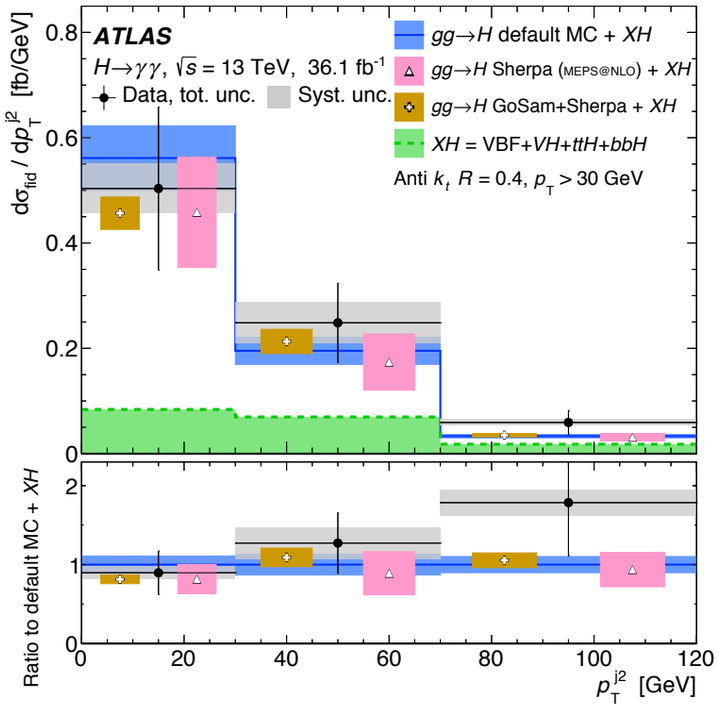

Total cross section - Channels combination

Acceptance factors

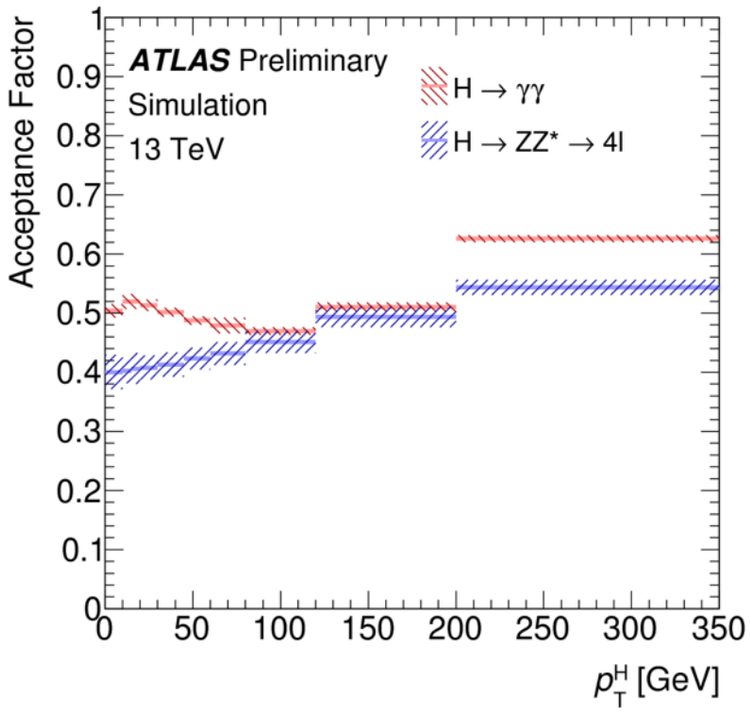

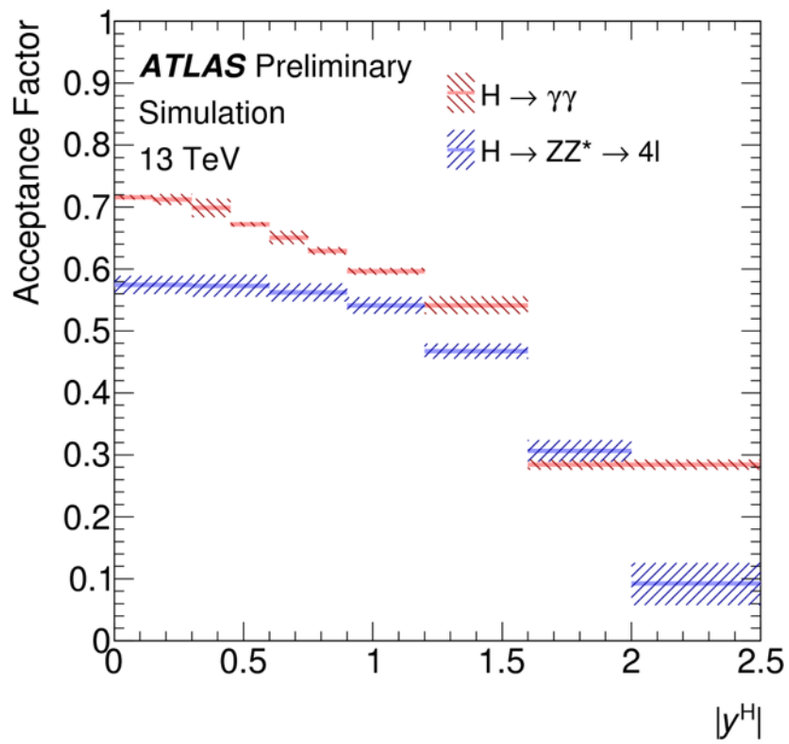

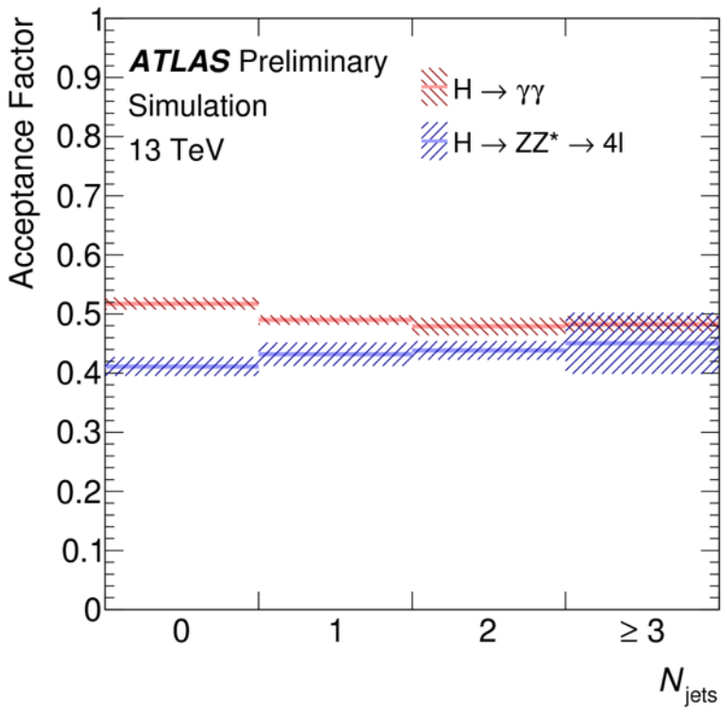

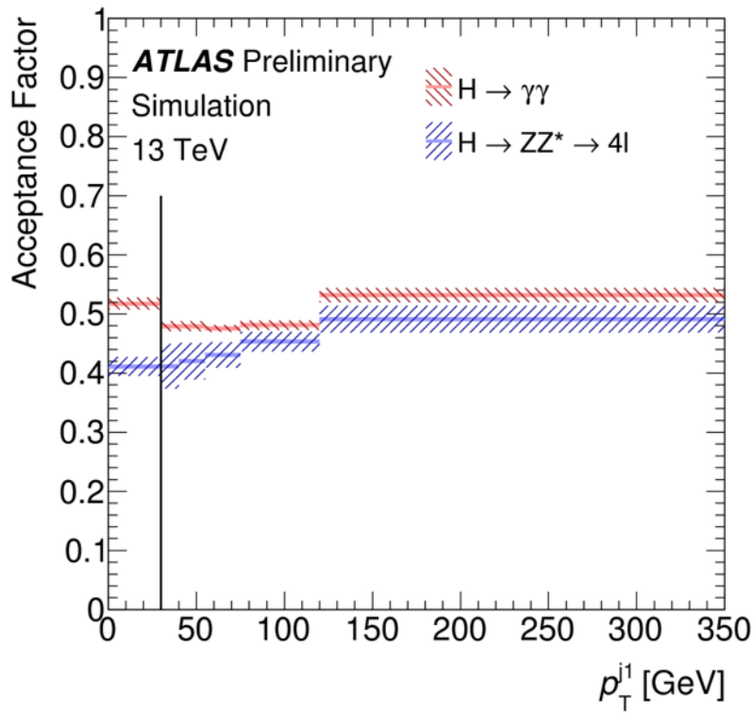

Total cross section - Channels combination

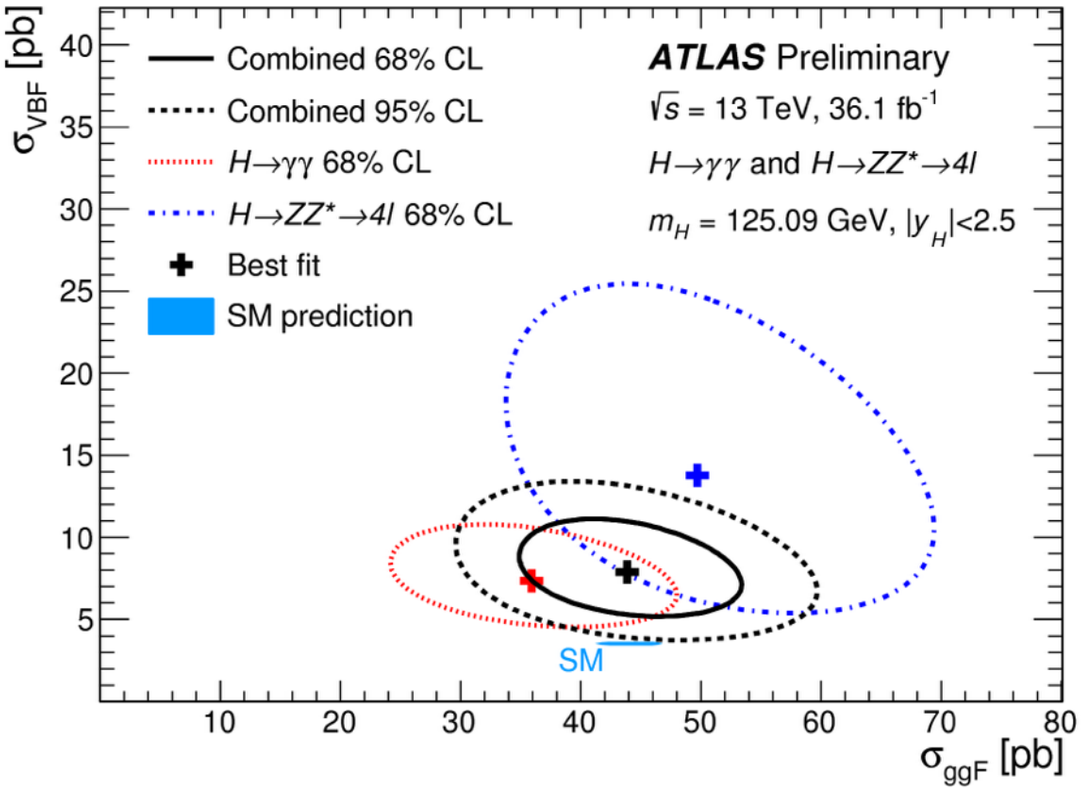

Both H->γγ and H->4l observe an anti-correlation between ggF and VBF measurements

Process ($\lvert y_H \rvert < 2.5$)	Result [pb]	Uncertainty [pb] Total	Stat.	Exp.	Th.	SM prediction [pb]
ggF	43.9	$^{+6.2}_{-6.0}$	$\left(^{+5.5}_{-5.4}\right.$	$^{+2.7}_{-2.3}$	$\left.\pm 1.2\right)$	$44.5^{+2.0}_{-3.0}$
VBF	7.9	$^{+2.1}_{-1.8}$	$\left(^{+1.7}_{-1.6}\right.$	$^{+0.8}_{-0.6}$	$\left.^{+1.0}_{-0.7}\right)$	$3.52^{+0.08}_{-0.07}$

Total cross section - Channels combination

Table 4: Leading uncertainties on the global signal strength. Signed impacts on μ are shown for a 1σ upward or downward shift on the uncertainty source, except in the cases of PDFs and branching fractions. The PDF uncertainty is dominated by PDF4LHC eigenvector 5, which decreases the signal strength by 0.018 due to a relative increase in the gluon distribution of 1.5% for a momentum fraction of $x = 0.01$ [68].

Source	Up	Down
Theoretical		
σ^{SM}_{ggF} (perturbative)	−0.045	+0.044
PDFs	±0.018	
Branching fractions	±0.014	
α_S	−0.011	+0.012
Experimental		
Luminosity	−0.037	+0.038
Energy resolution (e, γ)	+0.021	−0.019
Pileup	+0.014	−0.015

Production cross-sections in 4l channel

σ×B measured in several dedicated mutually exclusive regions of the phase space based on the production process. Production bins are chosen in such a way that the measurement precision is maximised and at the same time possible BSM contributions can be isolated.

- *simple fiducial region definitions for each Higgs production mode* based on Higgs kinematics and associated particles → match experimental categories

Advantage: cross-sections can be interpreted in terms of Higgs boson couplings, and theory uncertainties enter only at that stage

Two sets
of production bins considered:
Stage 0 (more inclusive ==> smaller statistical uncertainty)
and Reduced Stage 1(*)
(smaller theoretical uncertainties)

- e.g. exclusive jet bins and $p_T H$

(*) too fine granularity for precise measurements in all STXS Stage-1 bins => merge some categories

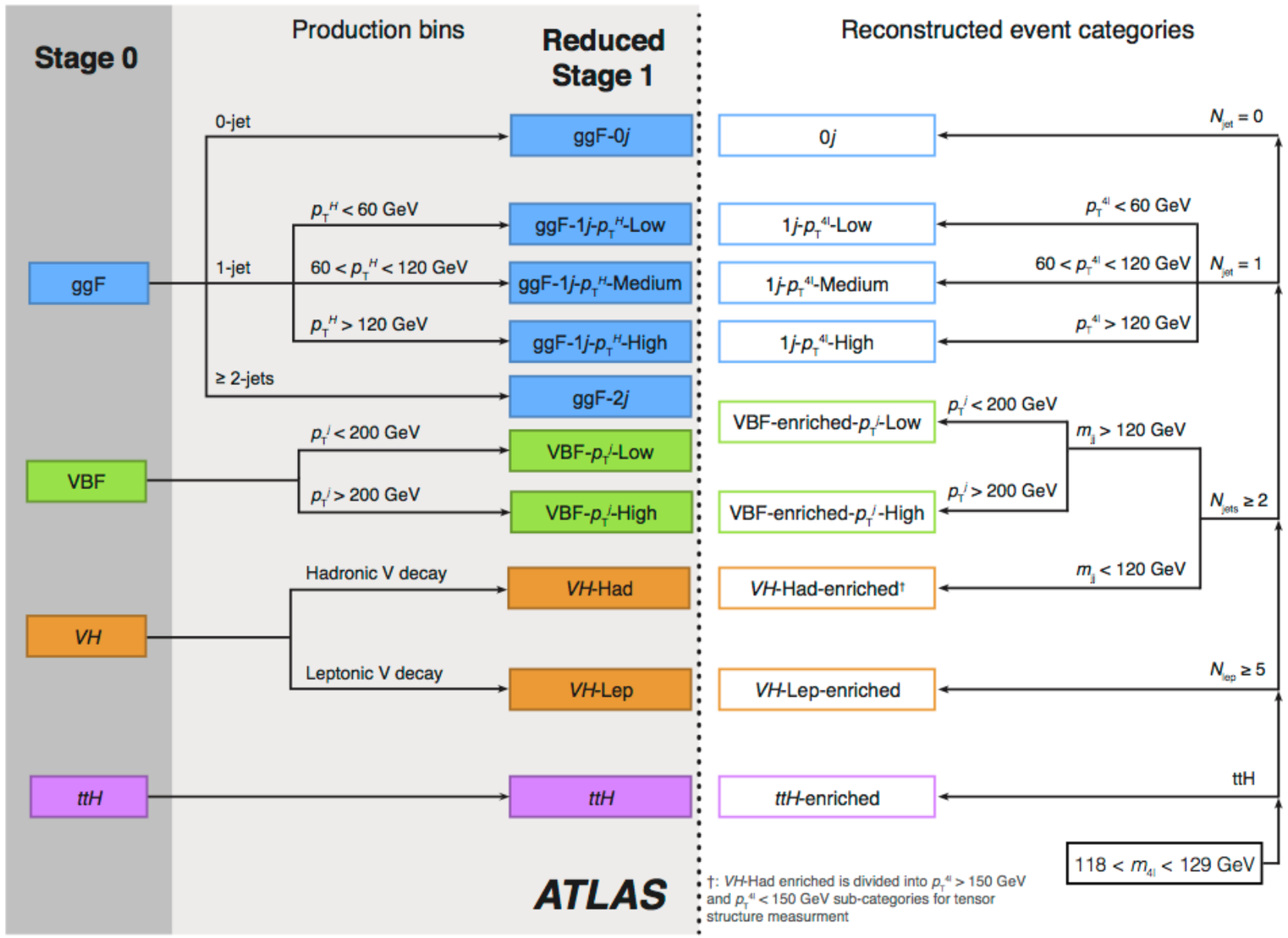

H→4l Stage-0 production cross-section measurements

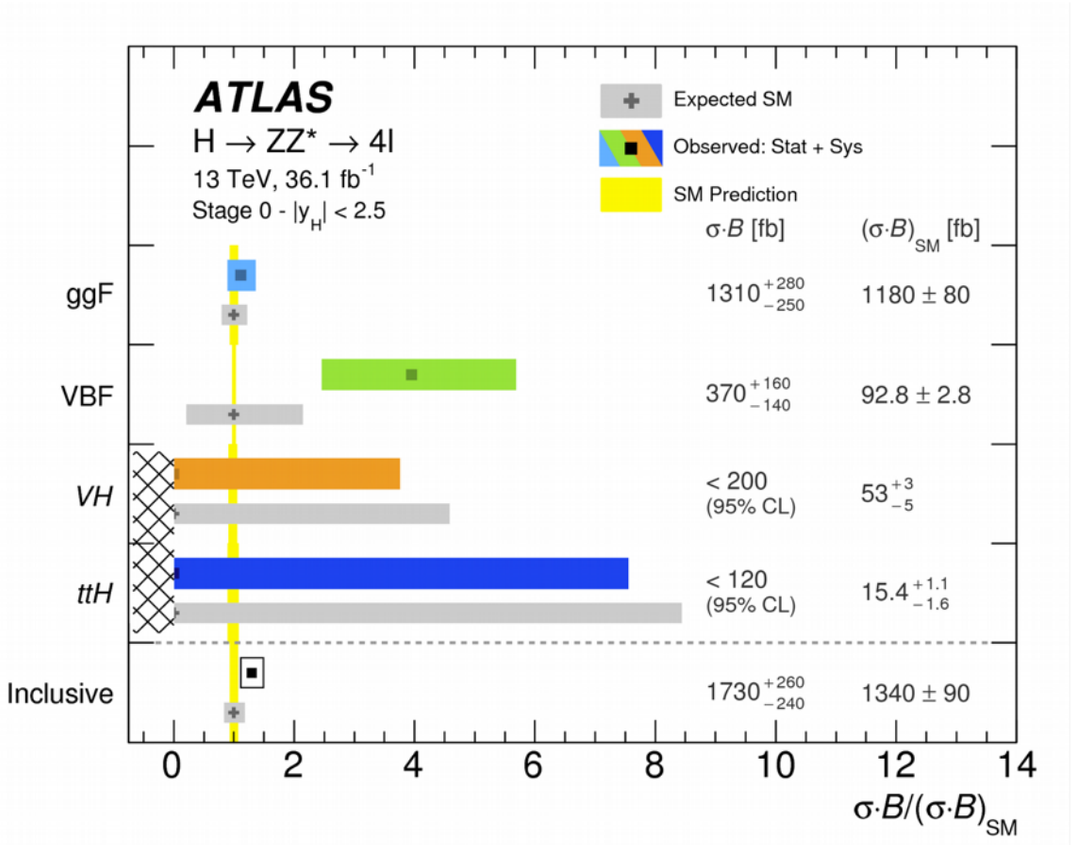

Combination of Stage-0 production cross-section measurements: Correlation matrix

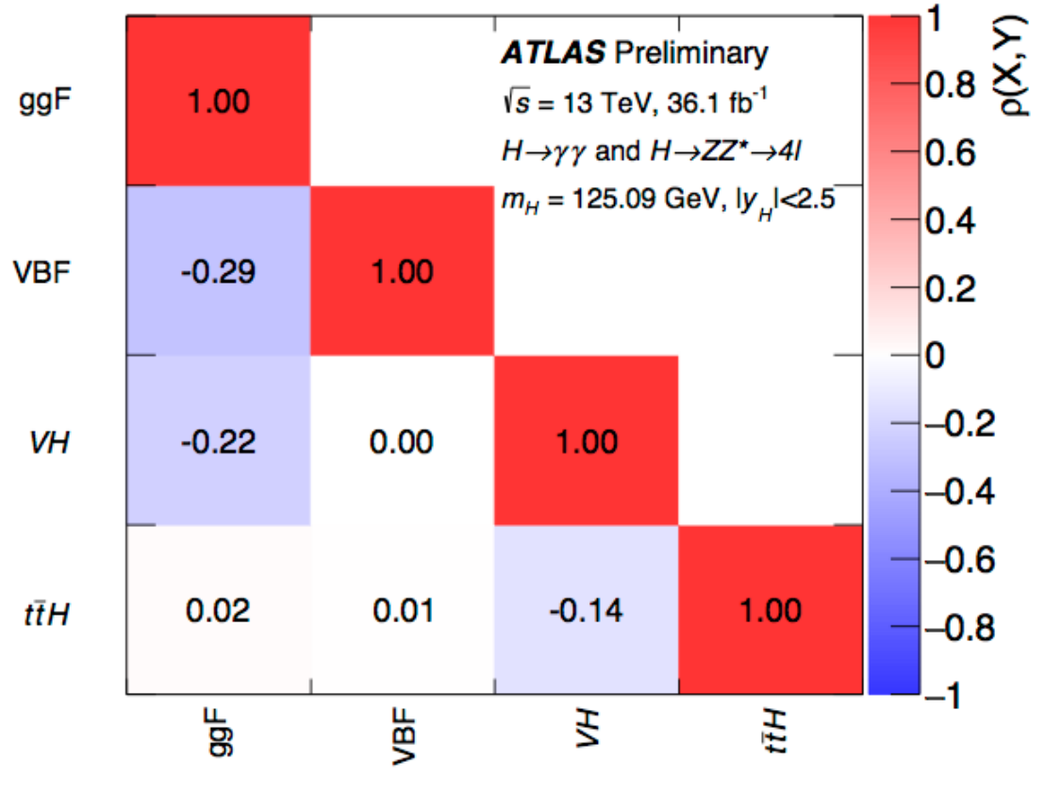

ggF and VBF anti-correlated since VBF category has large contribution from ggF production

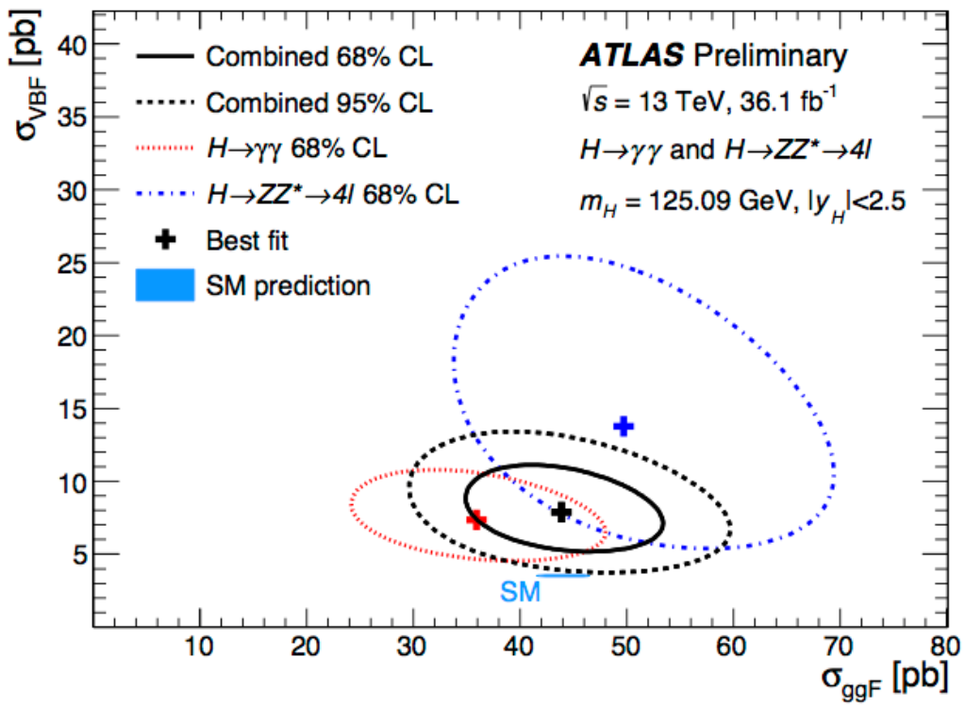

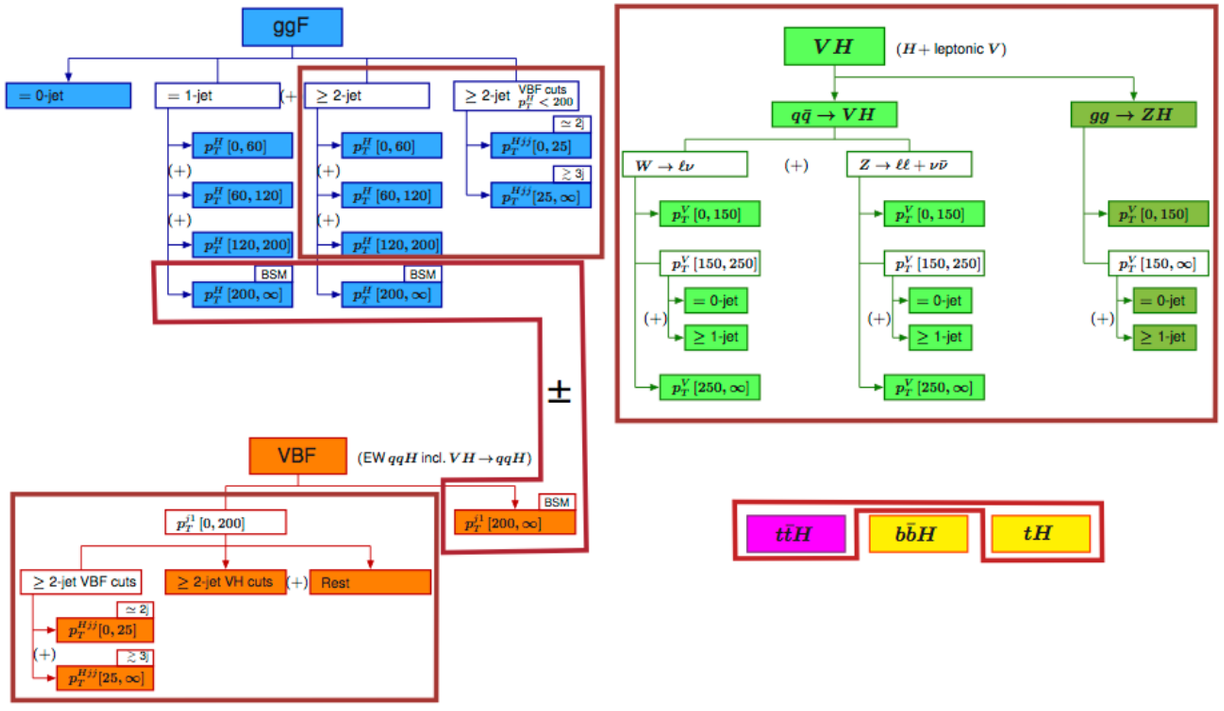

Stage-1 and bins merging
for intermediate Stage-1 ATLAS
measurements

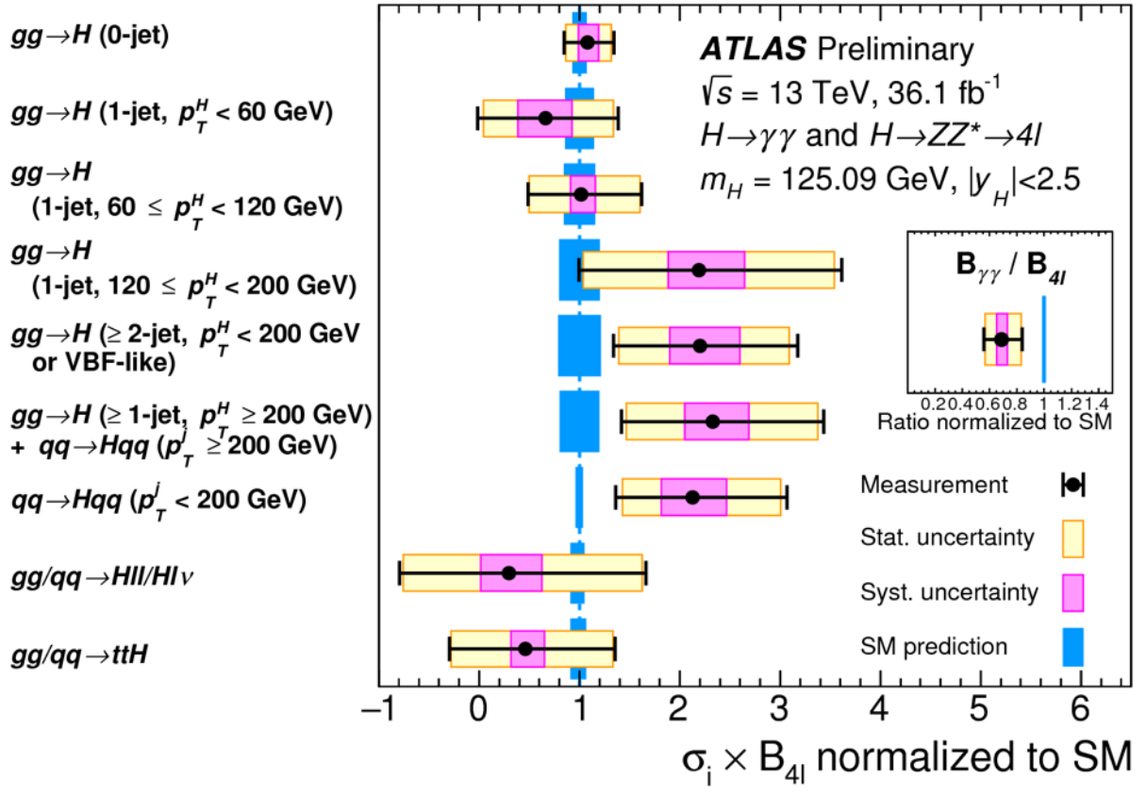

Towards Stage-1 Template XS measurement:
9 categories

Production cross-sections in γγ channel

The events satisfying the diphoton selection classified into 31 exclusive categories that are optimized for the best separation of the Higgs boson production processes and for the maximum sensitivity to the phase space regions defined by the stage 1 of the simplified template cross-section framework. A combined fit to the event reconstruction categories is then performed to determine nine simplified template cross sections (with |yH|< 2.5).

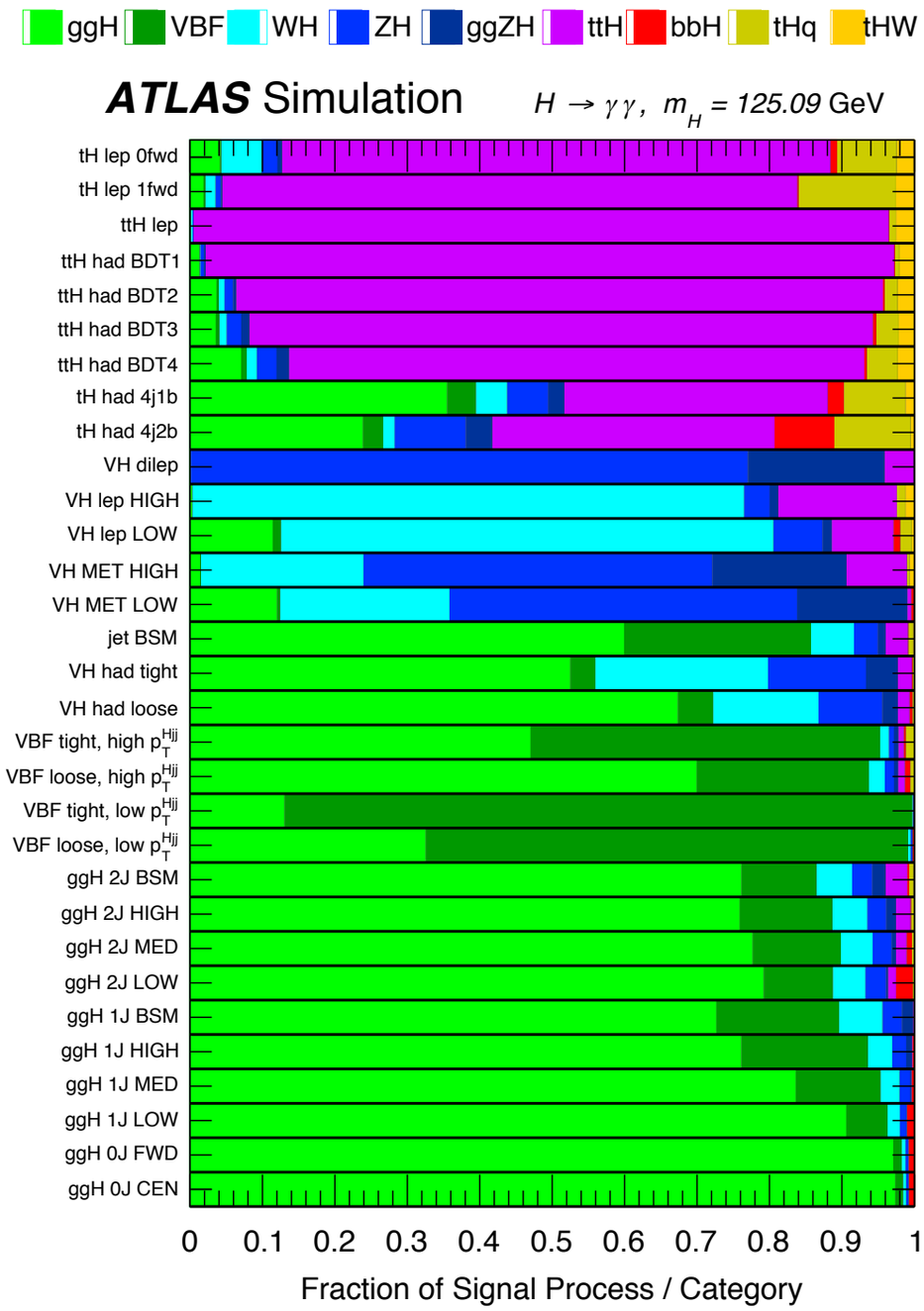

No sensitivity to all the 31 categories
==>
merge categories and fit in only 10/31 final categories

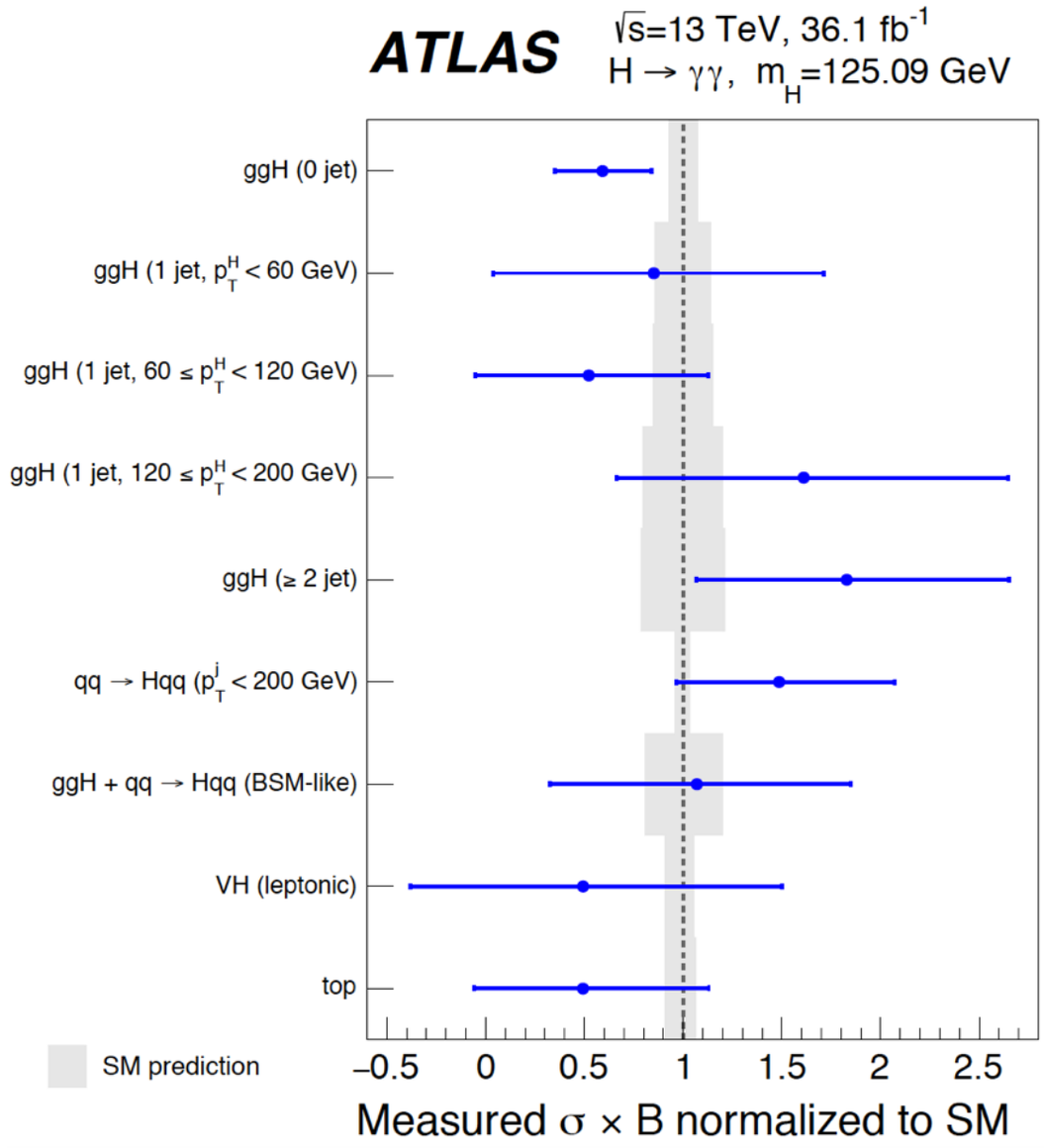

Production cross-sections in γγ channel

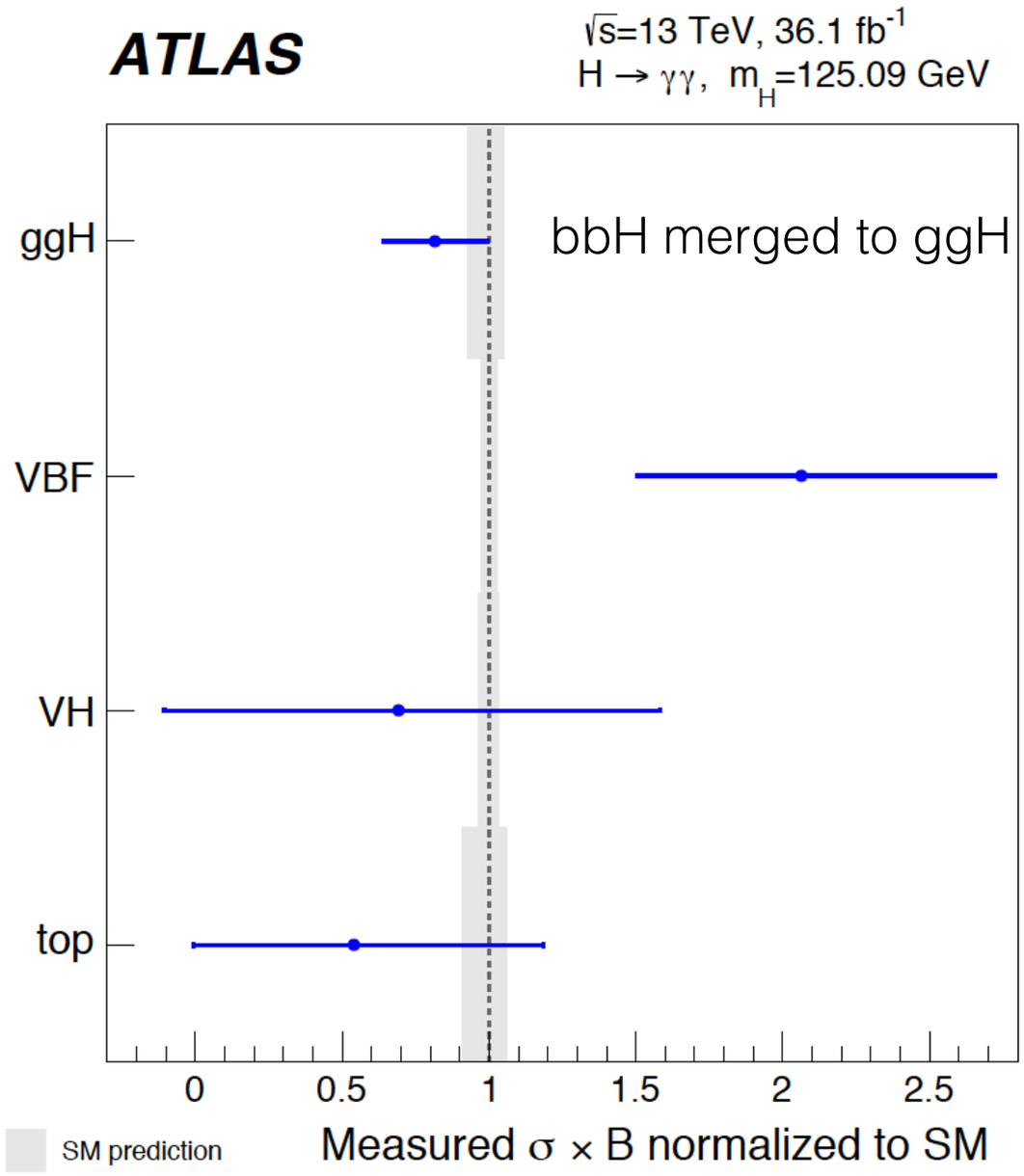

Measurements agree with SM predictions within 2σ

In general, all main production modes can be probed in diboson decays

68% and 95% CL 2D counters VBF vs ggF top and VH profiled in the fit

Higgs boson couplings

The Higgs boson couplings to heavy SM vector bosons (W and Z) and gluons are studied by measuring the cross sections for different production modes. The reconstructed Higgs boson candidate events are classified into different categories.
The categories are defined to be sensitive to different Higgs boson production modes, which in turn also provides sensitivity to the BSM contributions

$$\sigma(i \to H \to f) = k_i^2 \sigma_i^{SM} \frac{k_f^2 \Gamma_f^{SM}}{k_H^2 \Gamma_H^{SM}}$$

Fermion vs vector boson couplings:
ggF ~ κ_f^2, VBF ~ κ_V^2
$B_{4l} \sim \kappa_V^2$,
$B_{\gamma\gamma} \sim f(\kappa_f^2, \kappa_f^2, \kappa_f \times \kappa_V)$ from loops
assume $\Gamma^H_{BSM} = 0$ and only κ_f and $\kappa_V \neq 1$

κ_γ and κ_g are effective loop couplings for ggF and $H \to \gamma\gamma$

BMS searches

https://arxiv.org/abs/1504.04018

The differential fiducial cross sections can be interpreted in the context of searches for physics beyond the SM.
Limits are set on modified Higgs boson interactions within the framework of pseudo-observables.
The couplings related to the contact interaction of the Higgs boson decay are considered, ε_L, ε_R, which modify, in a flavour-universal way, the contact terms between the Higgs boson, the Z boson, and left- or right-handed leptons.
These contact terms only affect the dilepton invariant mass (not the lepton angular distribution) ==> The difference in $\chi 2$ between the measured and predicted cross sections in the m12 vs m34 observable plane is therefore used to constrain the possible contributions from contact interactions.

modifies the coupling between the Higgs boson and the Z boson

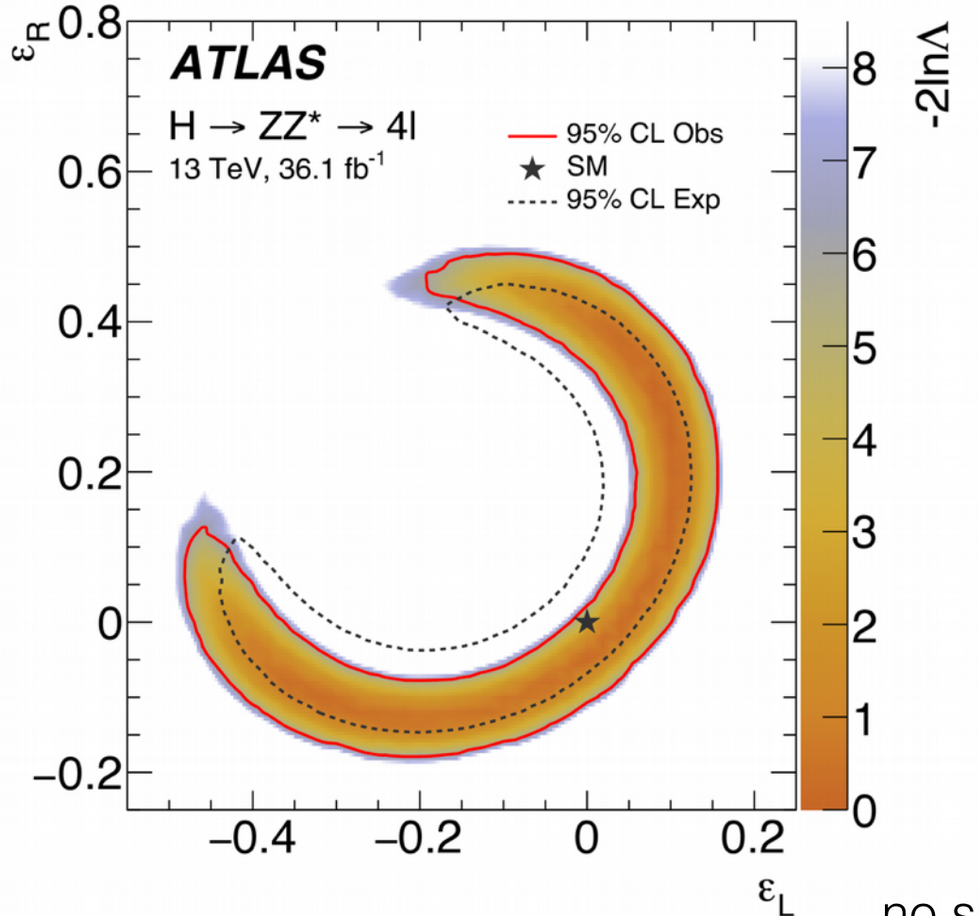

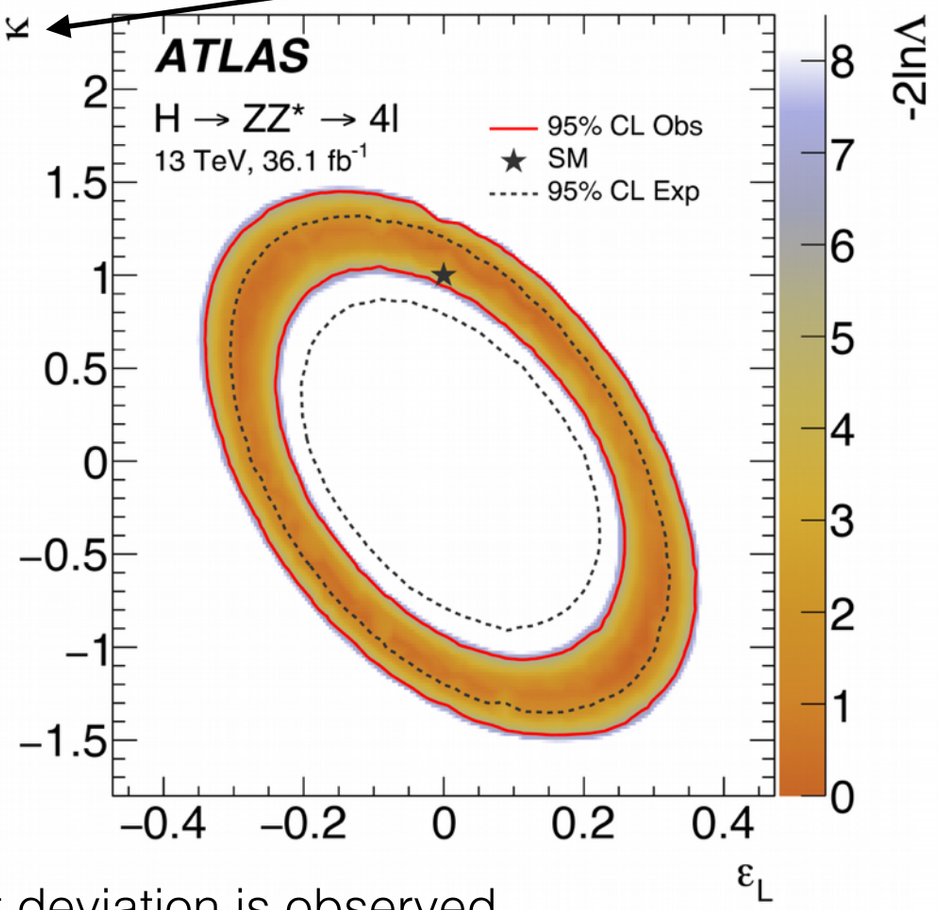

no significant deviation is observed

Higgs boson mass - 4l channel

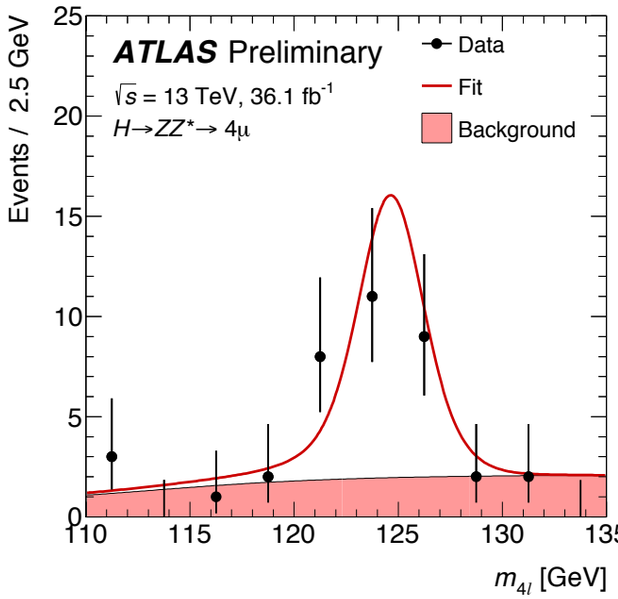

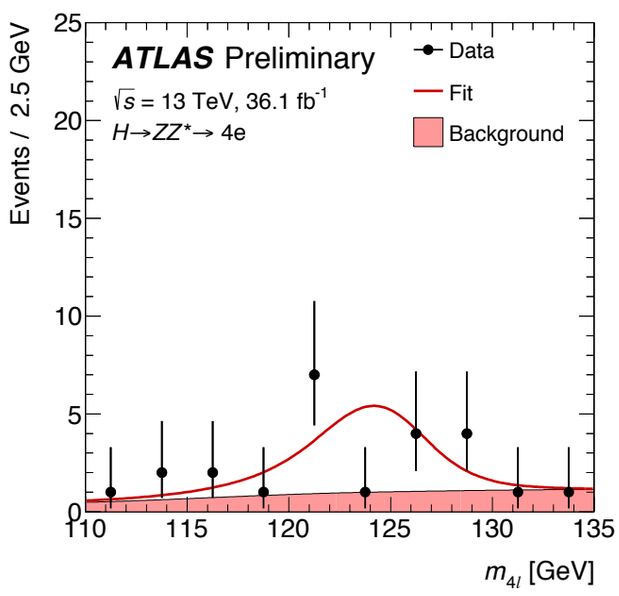

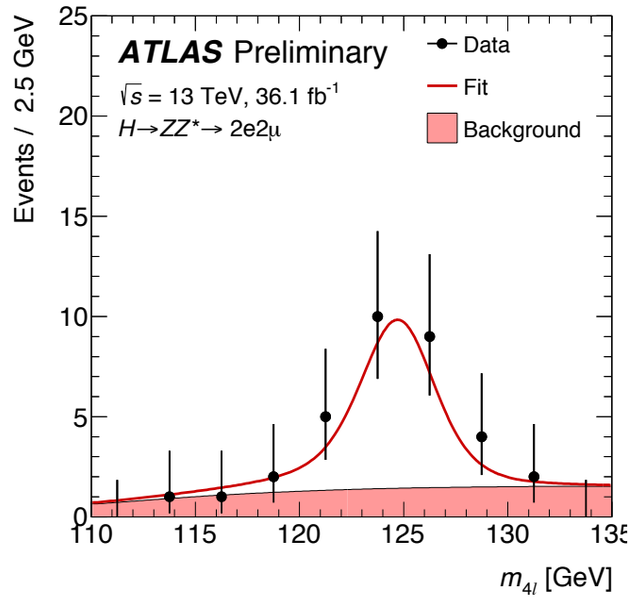

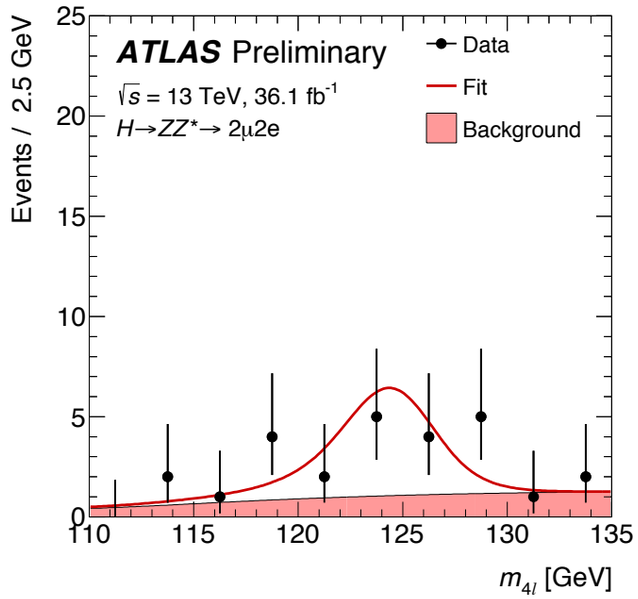

$$S_{m_H}(m_{4\ell}^{\text{meas}}) = \int_0^{\infty} F(m_{4\ell}^{\text{meas}} - m_{4\ell}^{\text{true}}) \cdot BW(m_{4\ell}^{\text{true}}, m_H)\, dm_{4\ell}^{\text{true}}.$$

Measured signal distribution as a convolution of the BW and a **response function F**

From simulation, using the lepton energy response functions (electron/muon and per detector region)
Depends on the lepton kinematics
==> the response functions combination for the 4l mass vary event-by-event

Final state	Signal (125 GeV)	ZZ^*	$Z+$jets, $t\bar{t}$, WZ, ttV,VVV	Expected	Observed
4μ	20.6 ± 1.7	15.9 ± 1.2	2.0 ± 0.4	38.5 ± 2.1	38
$2e2\mu$	14.6 ± 1.1	11.2 ± 0.8	1.6 ± 0.4	27.5 ± 1.4	34
$2\mu 2e$	11.2 ± 1.0	7.4 ± 0.7	2.2 ± 0.4	20.8 ± 1.3	26
$4e$	11.1 ± 1.1	7.1 ± 0.7	2.1 ± 0.4	20.3 ± 1.3	24
Total	57 ± 5	41.6 ± 3.2	8.0 ± 1.0	107 ± 6	122

Systematic effect	Uncertainty on $m_H^{ZZ^*}$ [MeV]
Muon momentum scale	40
Electron energy scale	20
Background modelling	10
Simulation statistics	8

σ(mass) ~ resolution
==> Z1 (leading pair) mass constraint
==> +15% improvement on m4l resolution

Higgs boson mass - γγ channel

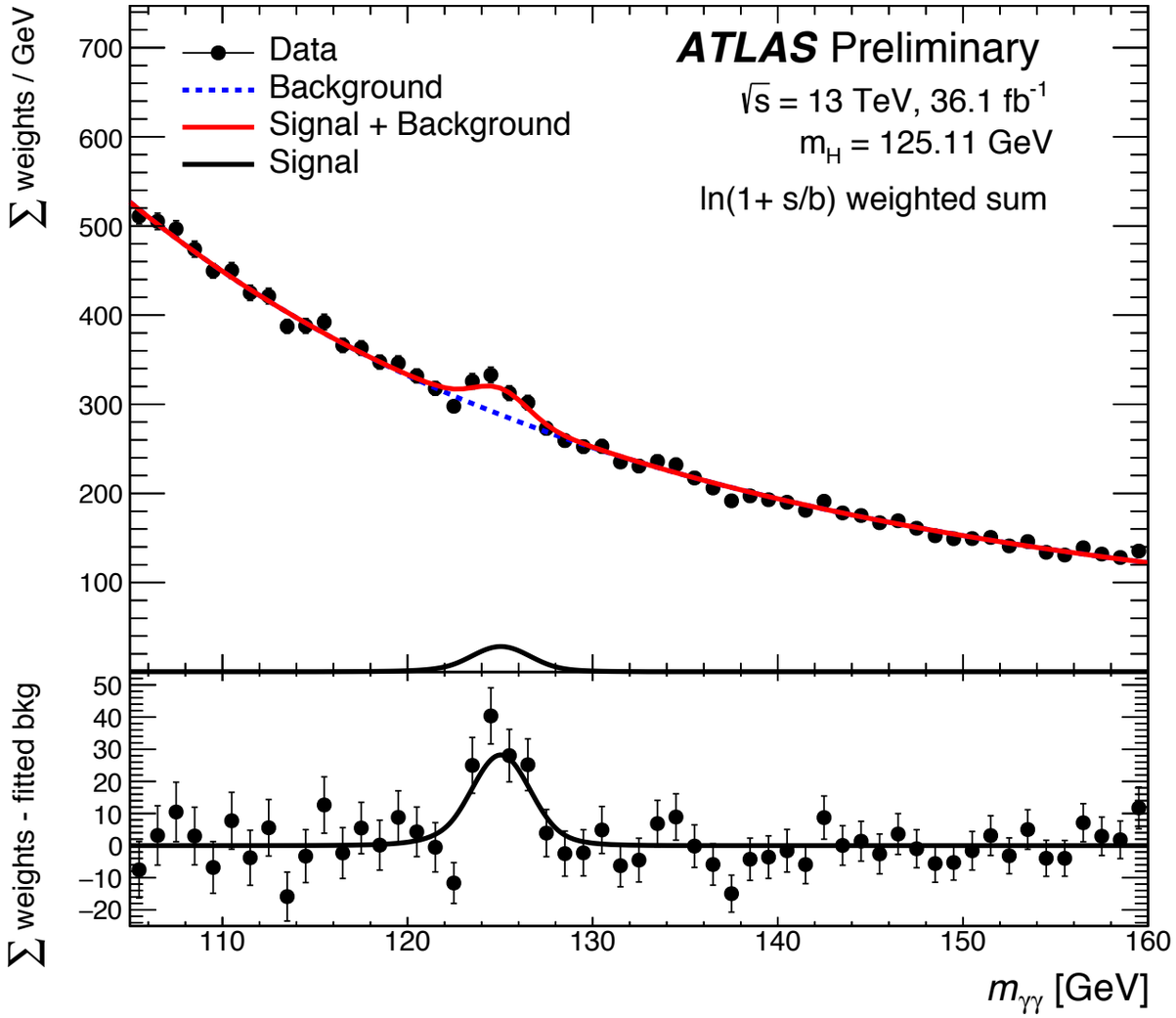

Systematic uncertainties breakdown

Source	Systematic uncertainty on $m_H^{\gamma\gamma}$ [MeV]
LAr cell non-linearity	±200
LAr layer calibration	±190
Non-ID material	±120
Lateral shower shape	±110
ID material	±110
Conversion reconstruction	±50
$Z \to ee$ calibration	±50
Background model	±50
Primary vertex effect on mass scale	±40
Resolution	$^{+20}_{-30}$
Signal model	±20

Anomalous couplings in EFT approach

The tensor structure of the Higgs boson couplings is studied, probing for admixtures of CP-even and CP-odd interactions in theories beyond the SM (BSM).
Use Effective Field Theory to search for deviations in the Higgs Lagrangian:

$$L_{EFT} = L_{SM} + \sum_i \frac{f_i}{\Lambda^2} O_i$$

EFT assume BSM particles above the cut-off Λ (=1TeV).
Introduce additional operators to the lagrangian

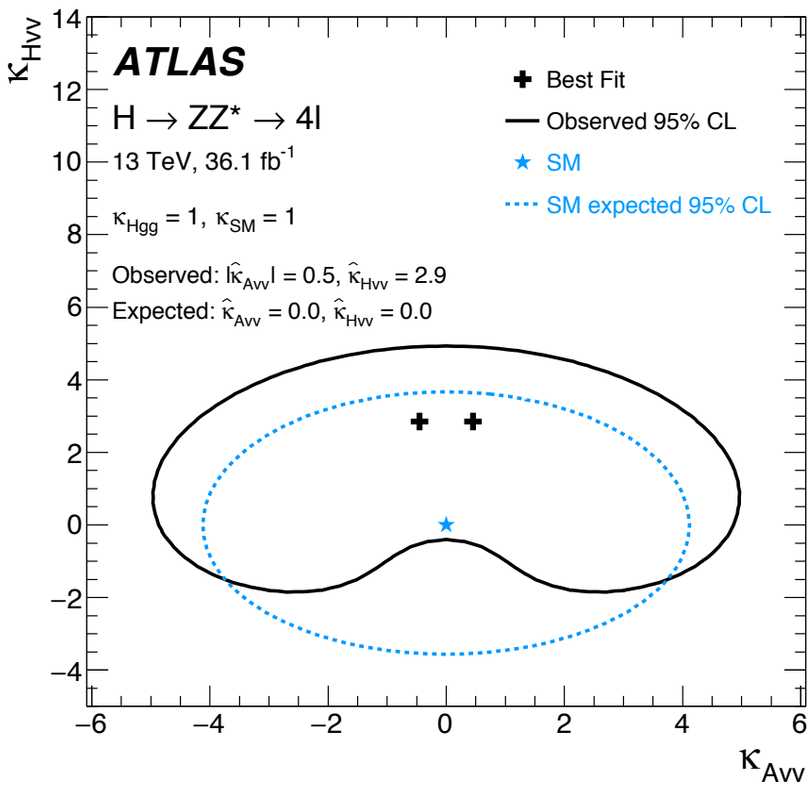

(a)

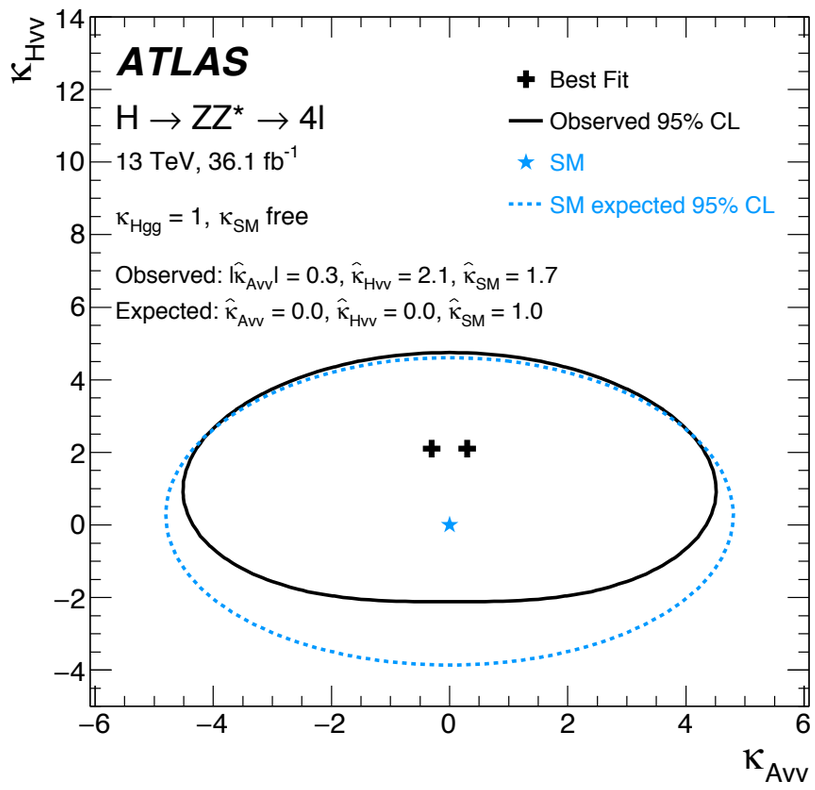

(b)

The CP-even and CP-odd BSM couplings to heavy vector bosons are also probed simultaneously

Figure 10: Observed (black) and SM expected (blue) contours of the two-dimensional negative log-likelihood at 95% CL for the κ_{HVV} and κ_{AVV} coupling parameters with 36.1 fb^{-1} of data at $\sqrt{s}$ = 13 TeV. The coupling κ_{Hgg} is fixed to the SM value of one in the fit. The coupling κ_{SM} is (a) fixed to the SM value of one or (b) left as a free parameter of the fit (b).

Spin/CP testing in γγ decays

The differential cross sections for $pp \to H \to \gamma\gamma$ as a function of $|\cos\theta^*|$ and $\Delta\phi_{jj}$ are shown in Figure 28. For a scalar particle $|\cos\theta^*|$, shows a strong drop around 0.6 due to the fiducial requirement on the photon system, whereas for a spin-2 particle, an enhancement would be present in precisely this region. The charge conjugation and parity properties of the Higgs boson are encoded in the azimuthal angle between the jets: For example, in gluon–gluon fusion, its distribution for a CP-even coupling has a dip at $\pm\frac{\pi}{2}$ and present peaks at 0 and $\pm\pi$, whereas for a purely CP-odd coupling it would present as peaks at $\pm\frac{\pi}{2}$ and dips at 0 and $\pm\pi$. For VBF the SM prediction for $\Delta\phi_{jj}$ is approximately constant with a slight rise towards $\Delta\phi_{jj}= \pm\pi$. Any additional anomalous CP-even or CP-odd contribution to the interaction between the Higgs boson and weak bosons would manifest itself as an additional oscillatory component, and any interference between the SM and anomalous couplings can produce distributions peaked at either $\Delta\phi_{jj}= 0$ or $\Delta\phi_{jj}= \pm\pi$ [138, 140, 141]. The shape of the distribution is therefore sensitive to the relative contribution of gluon–gluon fusion and vector-boson fusion, as well as to the tensor structure of the interactions between the Higgs boson and gluons or weak bosons. This is exploited in Section 9.5.8 to set limits on new physics contributions. To quantify the structure of the azimuthal angle between the two jets, a ratio is defined as

$$A_{|\Delta\phi_{jj}|} = \frac{\sigma(|\Delta\phi_{jj}| < \frac{\pi}{3}) - \sigma(\frac{\pi}{3} < |\Delta\phi_{jj}| < \frac{2\pi}{3}) + \sigma(|\Delta\phi_{jj}| > \frac{2\pi}{3})}{\sigma(|\Delta\phi_{jj}| < \frac{\pi}{3}) + \sigma(\frac{\pi}{3} < |\Delta\phi_{jj}| < \frac{2\pi}{3}) + \sigma(|\Delta\phi_{jj}| > \frac{2\pi}{3})},$$

which is motivated by a similar ratio presented in Ref. [140]. The measured ratio in data as determined by measuring $|\Delta\phi_{jj}|$ in three bins is

$$A^{\text{meas}}_{|\Delta\phi_{jj}|} = 0.45^{+0.18}_{-0.24}\,(\text{stat.})\,^{+0.10}_{-0.11}\,(\text{syst.})\,.$$

This value can be compared to the SM prediction from the default MC simulation. The predicted value is $A^{\text{SM}}_{|\Delta\phi_{jj}|} = 0.44 \pm 0.01$, consistent with the measured ratio.

In summary, the measured $|\cos\theta^*|$ and $\Delta\phi_{jj}$ distributions are consistent with Standard Model predictions for a CP-even scalar particle.